REPUBLIC OF TURKEY

ALTINBAŞ UNIVERSITY

Institute of Graduate Studies

Information Technology

DETECTION AND CLASSIFICATION OF BRAIN TUMORS IN MRI IMAGES USING DEEP CONVOLUTIONAL NEURAL NETWORK

Hussein ALISMAEELI

Master's Thesis

Supervisor

Prof. Dr. Osman Nuri UÇAN

Istanbul, 2022

DETECTION AND CLASSIFICATION OF BRAIN TUMORS IN MRI IMAGES USING DEEP CONVOLUTIONAL NEURAL NETWORK

Hussein ALISMAEELI

Information Technology

Master's Thesis

ALTINBAŞ UNIVERSITY

2022

The thesis titled “DETECTION AND CLASSIFICATION OF BRAIN TUMORS IN MRI IMAGES USING DEEP CONVOLUTIONAL NEURAL NETWORK” prepared by HUSSEIN LAYTH GHAZI and submitted on 16/12/2022 has been **accepted unanimously** for the degree of Master of Science in Information Technology.

Prof. Dr. Osman Nuri UÇAN

Supervisor

Thesis Defense Committee Members:

Prof. Dr. Osman Nuri UÇAN	Department of Engineering and Architecture, Altınbaş University	_____
Asst. Prof. Dr. Abdullahi Abdu IBRAHIM	Department of Engineering and Architecture, Altınbaş University	_____
Assoc. Prof. Dr. Adil Deniz DURU	Department of Sport Sciences, Marmara University	_____

I hereby declare that this thesis meets all format and submission requirements of a Master’s thesis.

Submission date of the thesis to Institute of Graduate Studies: ___/___/___

I hereby declare that all information/data presented in this graduation project has been obtained in full accordance with academic rules and ethical conduct. I also declare all unoriginal materials and conclusions have been cited in the text and all references mentioned in the Reference List have been cited in the text, and vice versa as required by the abovementioned rules and conduct.

Hussein LAYTH GHAZI ALISMAEELI

Signature

ABSTRACT

DETECTION AND CLASSIFICATION OF BRAIN TUMORS IN MRI IMAGES USING DEEP CONVOLUTIONAL NEURAL NETWORK

Alismaeeli, Hussein Layth Ghazi

M.Sc., Information Technology, Altınbaş University,

Supervisor: Prof. Dr. Osman Nuri UÇAN

Date: December/2022

Pages: 59

Brain tumors is a chronic and inflammatory disease of the central nervous system (CNS), which causes white matter lesions in the brain and spinal cord, as a result of demyelination of axons The brain tumors. can be classified into four types: Remissive-recurrent (RRMS), Secondary Progressive (EMPS), Primary Progressive (PPME) and Recurrent Progressive (PRMS) Recent work in Machine Learning (Machine Learning) and Deep Learning (Deep Learning) has shown fruitful outcomes, as observed in clinical applications and medical image processing Manual segmentation of lesions on magnetic resonance images has become the standard despite being labour-intensive and subject to interobserver variability (e.g., interobserver variability) In this thesis, we aimed to test out these two novel CNN implementations in the hopes of noticing performance gains. Our approach differs from those of others in that we use a multi-layer CNN rather than the standard three-layer architecture (convolution + subsampling + classification). In order to automatically segment sclerotic lesions in a magnetic resonance image, it is necessary to: investigate the existing literature containing models for this task; detail the primary procedures involved in pre-processing the image. Evaluate MRI lesion segmentation strategies based on

Convolutional neural networks; Incorporate a technique for automatic segmentation of lesions in MRIs of MS patients using magnetic resonance imaging analysis.

Keywords: MRI. BRAIN TUMOR, CNN, CNS, CAD.

TABLE OF CONTENTS

Pages

ABSTRACT ..... **v**

LIST OF FIGURES ..... **ix**

ABBREVIATIONS ..... **xi**

1. INTRODUCTION **1**

1.1 BACKGROUND 1

1.2 MOTIVATION 2

1.3 PROBLEM STATEMENT 3

1.4 CONTRIBUTION AND OBJECTIVES 4

1.4.1 Contributions 4

1.4.2 Objectives 4

1.5 THESIS ORGANIZATION 5

2. LITERATURE REVIEW **6**

2.1 CHAPTER OVERVIEW 6

2.2 PREVIOUS WORKS 6

2.3 CHAPTER SUMMARY 9

3. MATERIALS AND METHODS **10**

3.1 CHAPTER INTRODUCTION 10

3.2 CENTRAL NERVOUS SYSTEM 10

3.2.1 The Spinal Cord 11

3.2.2 The Brain 11

3.2.3 The Main CNS Substances 13

3.2.4 The Brain at The Cellular Level 14

3.2.5 Neurons 14

3.2.6 Cerebral Pathologies and Tumors 15

3.3 COMPUTER VISION SYSTEM 18

3.3.1 Magnetic Reasoning Images MRIs 19
3.4 BRAIN TUMORS MRI DATASET 22
3.5 DEEP LEARNING 23
3.5.1 Artificial Neural Networks 27
3.5.2 Convolutional Neural Networks 29
4. PROPOSED METHOD 32
4.1 U-NET 32
4.2 IMAGE ACQUISITION AND PRE-PROCESSING 32
4.2.1 Normalization 33
4.2.2 Histogram Equalization 33
4.3 SEGMENTATION USING CNN 34
4.4 CLASSIFICATION OF SEGMENTS 39
5. CONCLUSION AND FUTURE WORK 41
5.1 CONCLUSION 41
5.2 DISCUSSION 41
5.3 FUTURE WORK 43
REFERENCES 46

LIST OF FIGURES

Pages

Figure 1.1: Worldwide mortality rates in brain tumors according to WHO. 2

Figure 1.2: Basic principle of brain segmentation in deep learning (Zhou et.al 2021) 3

Figure 3.1: Human central nervous system..... 11

Figure 3.2: Human brain sections 12

Figure 3.3: Brain Tumor Types in different modalities 16

Figure 3.4: 3D MRIs of the human brain..... 19

Figure 3.5: Computer Aided detection CAD in MRIs 20

Figure 3.6: Example of Brain Tumors in different modalities..... 21

Figure 3.7: Brats dataset 22

Figure 3.8: Deep Learning position in the AI hierarchy 24

Figure 3.9: Deep learning feature optimization 25

Figure 3.10: ANN Structure..... 28

Figure 3.11: Artificial Neuron 29

Figure 3.12: Convolution Process in Artificial neural network 31

Figure 4.1: Nomadized Image vs non normalized image 33

Figure 4.2: Histogram equalization applied w 34

Figure 4.3: Feature Extraction by CNN. 35

Figure 4.4: Segmentation Using CNN model 36

Figure 4.5: Whole System steps summarized 37

Figure 4.6: An Example result 39

ABBREVIATIONS

SVM	:	Support Vector Machine
RRMS	:	Remissive-Recurrent
PPME	:	Primary Progressive
CNS	:	Central Nervous System
CAD	:	Computer Aided Detection
(MG),	:	Matter Gray
MRI	:	Magnetic Resonance Imaging

1. INTRODUCTION

1.1 BACKGROUND

brain tumors in the world are the leading cause of death in the world it is estimated that 17.9 million people died from brain tumors in 2019, which represents 32% of the number of deaths worldwide (World Health Organization, 2021). The most common method for disease detection is analysis, which includes clinical cardiac auscultation using a stethoscope (Mustafa et al., 2020). The stethoscope allows the heart to identify information such as heart rhythm, such and other professional heart anomalies. With the advancement of technology, stethoscopes improved, mainly, in the gain of the captured children. Currently, the digital stethoscope is available to specialists, which amplify sound and reduce noise, allowing the user's perception in more accurate diagnoses [1] The auscultation process is directly related to the MRI, which is a different graphic representation of the children originated by the heart and its great vessels. In this way, the detection of heart anomalies can be performed through the analysis of MRI videos, which allows the patient to the posterior, another method used in brain screening is the Electrocardiogram (EEG), which is a test that records the electrical activity of the heart. It is considered one of the methods of choice for detecting cardiac anomalies, since any event is reflected at the electrical level. at the level of emergencies and urgency, as well as a frequent routine examination. Its unparalleled quick, easy, and versatile advantage with auscultation is less cost-effective, more hardware-demanding, and difficult to implement in neonates with our digital and long resource of smartphones and topic stethoscopes, MRI has a lot of use throughout the literature. processes and suppress existing ones.

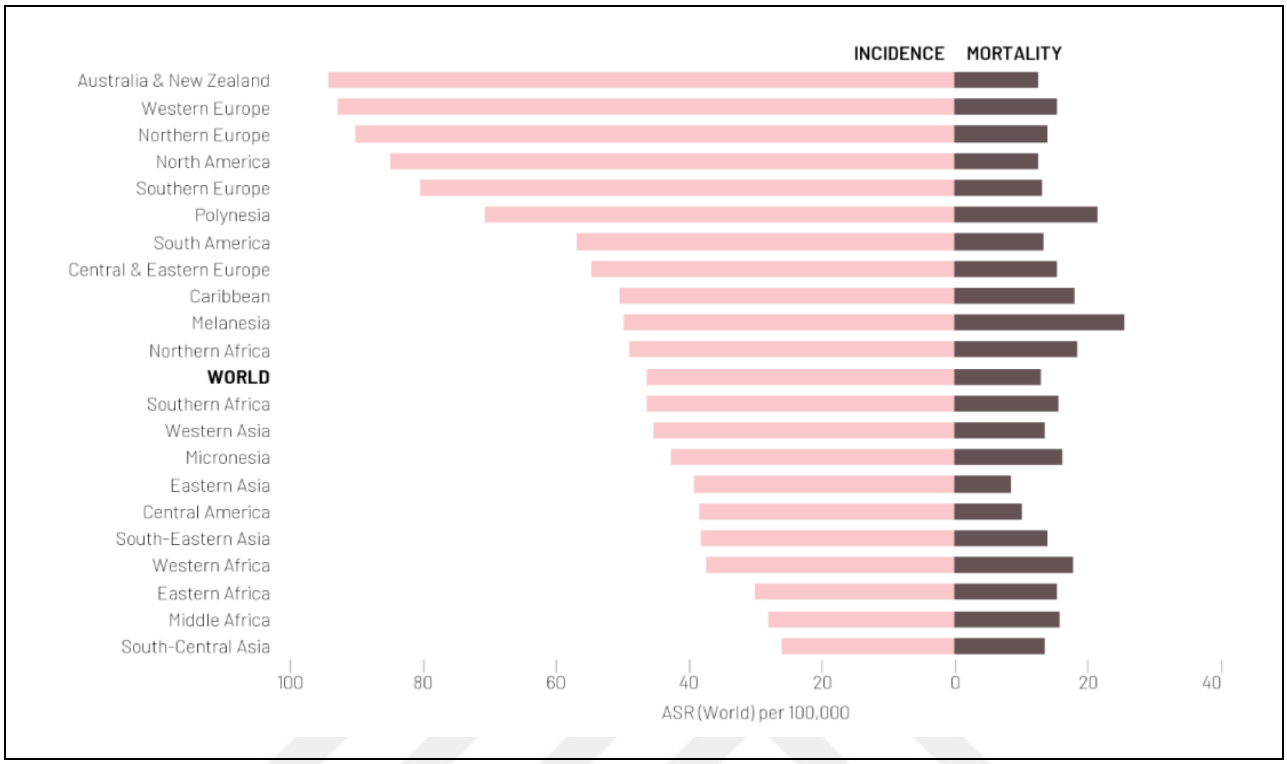

Figure 1.1: Worldwide mortality rates in brain tumors according to WHO.

1.2 MOTIVATION

Brain tumor is a chronic and inflammatory disease of the central nervous system (CNS), which causes white matter lesions in the brain and spinal cord, as a result of demyelination of axons [1]. Myelin is a substance that surrounds the axon, forming an electrically insulating layer, having a fundamental role in the communication between neurons, facilitating the transmission of electrical signals [2]. From the demyelination process, there is formation of fibrous tissue around the lesions (gliosis) [3]. The location of the CNS affected by these lesions influences the pathological features of the disease [4]. Clinically, Multiple Sclerosis presents great variability of manifestations, which can affect mobility, balance, vision and cognition [5]. The brain tumors. can be classified into four types: Remissive-recurrent (RRMS), Secondary Progressive (EMPS), Primary Progressive (PPME) and Recurrent Progressive (PRMS) [6] From a radiological point of view, the demyelination process can be visualized through the image of MRI.

1.3 PROBLEM STATEMENT

Because of its extraordinary capacity to detect disease-related lesions even in the absence of symptoms, magnetic resonance imaging (MRI) is the imaging tool most commonly employed to diagnose brain malignancies [7]. Manual segmentation of lesions on magnetic resonance images has become the standard despite being labour-intensive and subject to interobserver variability (e.g., interobserver variability). [9]. Recent work in Machine Learning (Machine Learning) and Deep Learning (Deep Learning) has shown fruitful outcomes, as observed in clinical applications and medical image processing [10]. [11] There has been considerable interest in the technique of automatically recognizing and segmenting multiple sclerosis-related lesions. These technologies can be utilized both within and outside of the classroom.

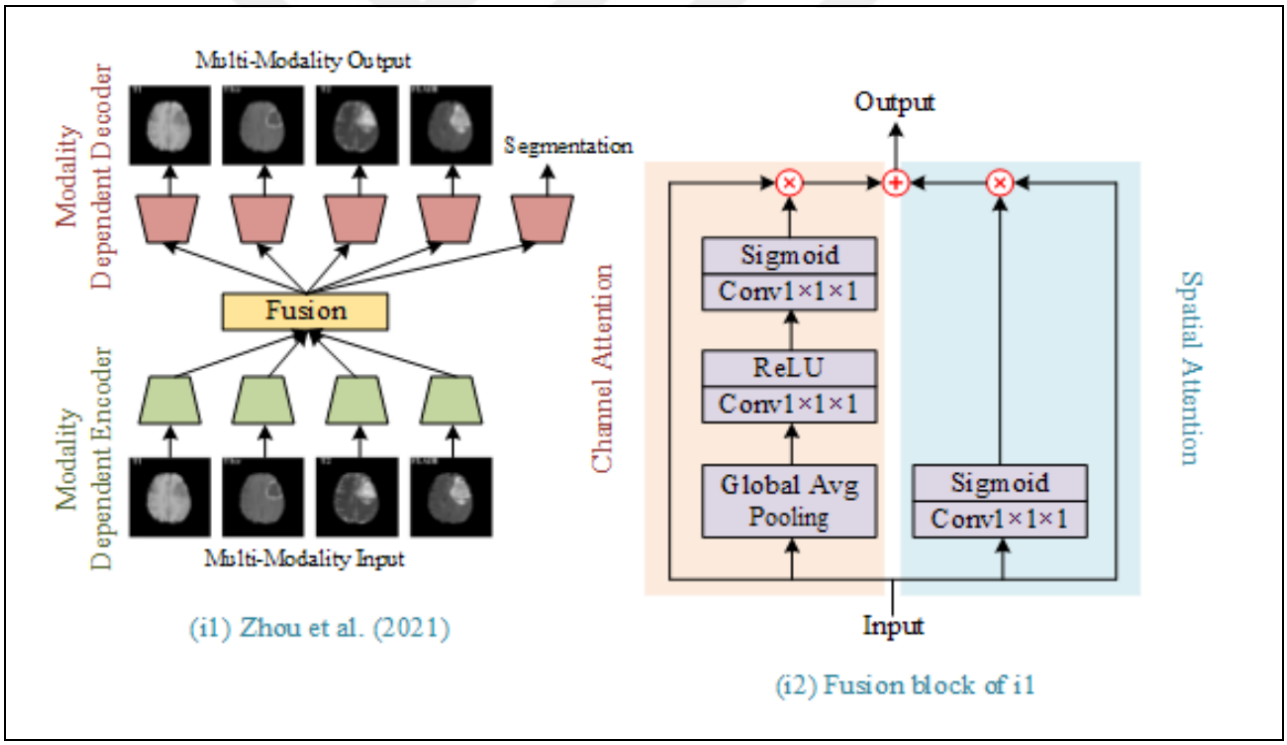

Figure 1.2: Basic principle of brain segmentation in deep learning (Zhou et.al 2021)

1.4 CONTRIBUTION AND OBJECTIVES

1.4.1 Contributions

In this thesis we wanted to experiment with both these innovative approaches to CNN, in the hope of observing improvements in performance. Unlike previous works, which uses a single level CNN consisting of a convolution layer and a subsampling layer and a classification layer at the end, we increase the depth by introducing a second layer. This master's thesis had the following contributions:

a) Explore the existing literature with models of segmentation of sclerotic lesions in the brain;

b) Explain the main steps of pre-processing of magnetic resonance image, in order to segment the lesions by automated means;

c) Analyze Convolutional Neural Networks techniques for segmentation of lesions in MRI;

d) Implement a magnetic resonance image analysis methodology for automatic segmentation of lesions in patients with Multiple Sclerosis.

1.4.2 Objectives

The goal of this thesis is the construction of a "Computer aided detection" (CAD) for the automatic segmentation of non-massive brain tumor. This would be of considerable use in the clinic because today the tumor is manually segmented by the radiologist: the use of a CAD would allow the process to be automated, making it extremely faster and also less affected by inter and intra operator variability. The CAD is built and evaluated on magnetic resonance images, through deep learning, and comparisons are made between different normalizations of the images of the dataset, different loss functions and binarizations of the masks predicted by the CAD, in such a way as to evaluate and compare the effects that the variation of these parameters affects the performance of the system.

1.5 THESIS ORGANIZATION

This thesis is divided into 6 chapters.

a) In this chapter, a contextualization of the theme and its problematic is made.

b) Chapter 2 presents the fundamentals of brain tumors in the previous works of literature.

c) Chapter 3 covers basic principles of MRI and imaging characterization of lesions.

d) Chapter 4 describes the computational methodology used in this study.

e) Chapter 5 presents the results obtained, followed by discussion.

f) Finally, chapter 6 presents the conclusions and recommendations for future work.

2. LITERATURE REVIEW

2.1 CHAPTER OVERVIEW

The purpose of this chapter is to provide a comprehensive technical evaluation of various deep learning-based brain tumor segmentation algorithms. This analysis will employ architectural classifications and strategy comparisons.

In this study, we intend to investigate how different neural network topologies affect the segmentation performance of deep neural networks and how different learning techniques can be improved for various barriers in brain tumor segmentation. We are specifically interested in how these characteristics influence the ability of deep neural networks to detect and categorize brain cancers.

We cover diverse high-level perspectives, including effective architecture design, imbalance segmentation and multi-modality process.

The taxonomy of this chapter is made such that our categorization can help the reader to understand the technical similarities and differences between segmentation methods. The proposed taxonomy may also enable the reader to identify open challenges and future research directions.

2.2 PREVIOUS WORKS

Deep Learning is a subset of Machine Learning, a subfield of Artificial Intelligence referred to as Machine Learning (AI). Researchers in the field of machine learning are interested in both the improvement of representations and the application of models to "learn" them. Their research focuses mostly on the subject of what makes a representation more accurate and how models might be created to "learn" it. Using approaches from the field of deep learning, we are able to simulate the functioning of the human visual brain. The human visual cortex functions similarly to a hierarchical filtering system in that it takes information from lower layers and transmits it to higher ones, where it is transformed.

Deep learning algorithms are a category of algorithms that use a deep architecture to attempt to model data on their own. This design consists of multiple layers of abstraction, and the concepts at the highest levels are dictated by the concepts at the lowest levels via a nonlinear transformation.

In recent years, it has been demonstrated that these methodologies outperform alternative approaches in a range of applications, including those involving image classification, recognition, and natural language processing. Google hired Geoffrey Hinton from the University of Toronto in March 2013, and Facebook hired Yann LeCun from New York University in December 2013. Both men had previously worked at Canadian universities.

In a 1996 study [11] employing the Convolutional Neural Networks method, which is a subfield of deep learning, Heang-Ping Chan exhibits positive results with regard to digital mammography image classification of healthy tissues and tissues bearing masses. According to the article, the primary purpose of this thesis is to continue and expand upon the work reported therein by employing a more complex architecture (consisting of multiple levels of representation) and new methodologies that have been previously applied to CNN in the study of other subjects. In CNNs, the convolution layer is commonly followed by a subsampling layer, and the subsampling layer is typically followed by a normal neural network that performs the final categorization of pictures following the application of filters (kernels). Subsampling an image often involves dividing the image into a number of nonoverlapping rectangles and then replacing the value of each rectangle with its respective mean.

Despite the lack of a theoretical basis, Jianchao Yang and colleagues [24] argue in a 2009 study that moving from the maximum operation to the average one improves classification performance for a wide range of objects and contexts. In many DL models, the final layer of the hierarchy for classification tasks consists of a standard neural network with a softmax activation function. This function is generally referred to as multinomial logistic regression.

Yichuan Tang [13] published an article titled "Deep Learning Using Linear Support Vector Machine" to demonstrate the effectiveness of using a support vector machine (SVM) as opposed to a neural network on popular datasets such as MNIST (a public database of handwritten figures), CIFAR-10 (ten classes of various Internet-sourced images), and ICML 2013 (a collection of machine learning benchmarks) (facial expression recognition).

Zhu et al. [2] started to use a Hopfield Neural Network with active contours to extract the tumor boundary and dilate the tumor region. However, training a neural network was highly constrained due to the computational resource limitation and technical supporting. From late 90s’ to early 20s’,

most of the brain tumor segmentation methods focused on traditional machine learning algorithms with hand-crafted features, such as expert systems with multispectral histogram [30], segmentation with templates [31], [32], graphical models with intensity histograms [33], [34], tumor boundary detection from latent atlas [35]. These early works pioneered the use of machine learning in solving brain tumor segmentation problems. However, early research works have significant shortcomings. First, most of the early works only focused on the segmentation of the whole tumor region, that is, the segmentation result has only one category. Compared with recent brain tumor segmentation algorithms, early works are formulated with strong conditions, relying on unrealistic assumptions. Second, manually designed feature engineering is constrained by prior knowledge, which cannot be fully generalised. Last but not least, early research works fail to address some challenges such as appearance uncertainty and data imbalance. With the revolutionary breakthrough by deep learning technology [36], researchers began to focus on using deep neural networks to solve various practical problems.

Pioneering works from Zikic et al.[37], Havaei et al.[38], Pereira et al.[39] intend to design customized deep convolutional neural networks to achieve accurate brain tumor segmentation. With breakthrough brought by Fully Convolutional Network (FCN) [40] and U-Net [41], recent innovations [42], [43] on brain tumor segmentation focus on building encoder-decoder networks without fully con nected layers to achieve end-to-end tumor segmentation. A long-standing challenge in brain tumor segmentation is data imbalance.

To effectively deal with the imbalance problem, researchers try different solutions, such as network cascade and ensemble [44], [45], [46], multi-task learning [47], [48], and customized loss functions [49]. Another solution is to fully utilise information from multimodality. Recent research focused on modality fusion [50] and dealing with modality missing [51]. Based on the evolution, we generally categorise the existing deep learning-based brain tumor segmentation methods into three categories, i.e., methods with effective architectures, methods for dealing with imbalanced condition and methods of utilising multi-modality information.

2.3 CHAPTER SUMMARY

When it comes to the classification of brain tumors, there are numerous unanswered questions. The objective of brain tissue segmentation, also known as anatomical brain segmentation, is to assign a certain category of brain tissue to each individual unit under study. To perform their responsibilities, they are functioning under the presumption that the brain imaging does not reveal any tumor tissue or other abnormalities.

Tumor detection is to identify aberrant tumors or lesions and communicate the tissue's expected classification. In this context, a bounding box is frequently used as a detection result, but a label is used for categorization purposes.

However, it is essential to remember that certain procedures for segmenting brain tumors provide only a single label mask or the central location of the tumor core without sub-regional analysis.

Survival Prediction is a method that, in addition to clinical diagnosis, identifies the patterns and activity of tumors to predict the patient's likelihood of survival [6, 11]. On the basis of the results of tumor segmentation, it is reasonable to consider disease classification and survival prediction as subsequent tasks. Both are essential components of cancer research.

3. MATERIALS AND METHODS

3.1 CHAPTER INTRODUCTION

In this first chapter, we will introduce the fundamental notions related to the context of our work. First, we will cover some notions of brain anatomy by defining the essential terms and concepts that allow us to better understand what we observe with brain imaging. Then, we will present the pathologies and the cerebral tumors in specific the glioma which constitutes approximately a third of the most frequent primitive cerebral tumors. And we will end this chapter with the principle of magnetic resonance imaging [MRI].

In this work we are developing a new deep learning method to identify and delineate tumors in medical images. The software automatically analyzes several medical image modalities. Through a self-learning process inspired by the functioning of neurons in the brain, it automatically identifies brain tumors, outlines the contours of the prostate for radiotherapy or counts the number of cells on a microscopic scale with a performance similar to the eye of a human expert. We developed software that could be integrated with visualization tools to help physicians with advanced analysis of different medical imaging modalities. The algorithm makes it possible to automate tasks of preprocessing, detection and segmentation – that is to say the delimitation – of images which are not currently carried out because it takes too much time for a human. Our model is very versatile, it works for computed tomography images [CT scan] of the brain, magnetic resonance images [MRI] of the prostate and images of cells in electron microscopy",

3.2 CENTRAL NERVOUS SYSTEM

The central nervous system is responsible for information processing (CNS). In addition to detecting signals from the outside world, it also records, analyzes, and organizes their responses. The spinal canal contains the spinal cord and nerves of the spinal column, whereas the cranial box contains the cerebrum, brainstem, and cerebellum [1]. Figure 3.1 depicts the various behaviors of the central nervous system (CNS) as follows: Following this, there are various sections in which we elaborate on each of these traits.

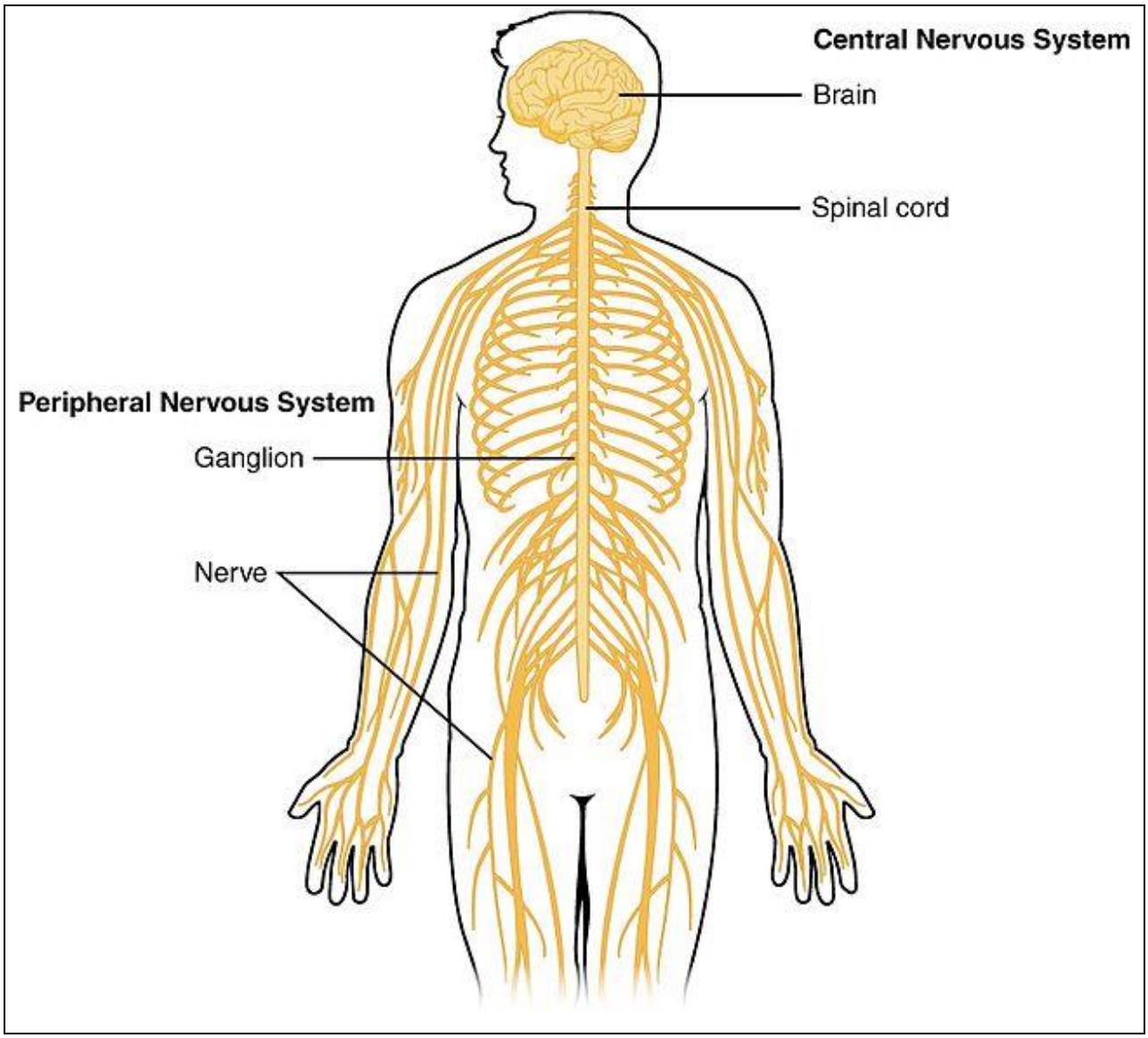

Figure 3.1: Human central nervous system

3.2.1 The Spinal Cord

This is a cord of nervous tissue located in the vertebral canal. It has two bulges: a cervical bulge and a lumbar bulge [2].

3.2.2 The Brain

The term "brain" refers to the portion of the nervous system that is housed within the cranium as well as the region at the base of the skull. Included in this are the cerebral hemispheres, the

cerebellum, and the brainstem. This structure is protected by the cerebrospinal fluid, which acts as a cushion for it. [CSF] [3].

A. Brainstem

The two hemispheres of the brain are connected to one another by connections that run from the brainstem to the spinal cord. This organ is responsible for regulating not just the heart and lungs but also the blood pressure. Amongst other duties, it is responsible for controlling eye movement and face movement, as well as swallowing [4].

B. Cerebellum

In the human body, the cerebellum is located in the very rear of the brainstem, immediately below the occipital lobes. This allows us to respond quickly, coordinate our actions, and maintain our equilibrium.[4].

C. Brain

It is divided into 2 cerebral hemispheres: right hemisphere and left hemisphere, each Hemisphere is divided into 4 lobes [figure 3.2]:

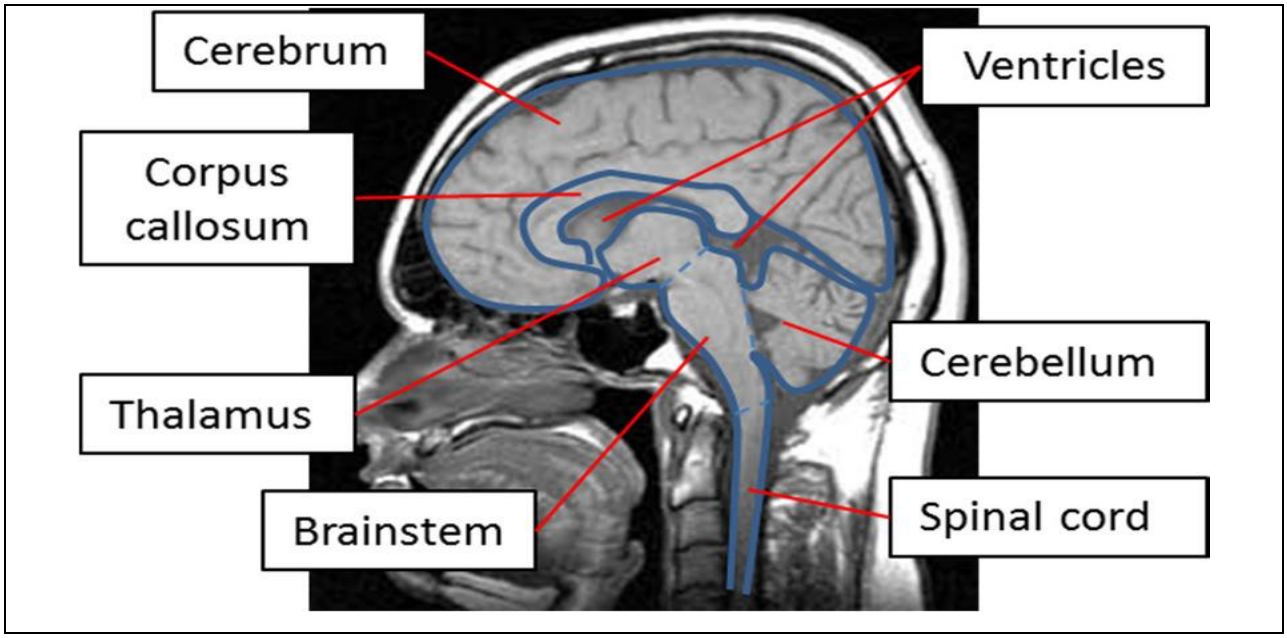

Figure 3.2: Human brain sections

a) The frontal lobe: involved in thinking, conceptualizing, planning, conscious appreciation of emotions.

b) The parietal lobe: involved in gestures, orientation and spatial recognition, calculation. • The occipital lobe: mainly the seat of vision.

c) The temporal lobe: dedicated to the interpretation of sounds, language and memory [5].

3.2.3 The Main CNS Substances

A. Gray matter

The cell bodies of neurons are represented by gray matter, often known as gray matter (MG), and this material contains a dense dendritic network. It is located in the cortex, which is a thin layer that covers the cerebellum and the rest of the brain [7].

B. White matter

The material in question is of a white color. MB, also known as white matter, refers to the myelin covering that surrounds the axons of neurons in the brain. Axons that have been myelinated create bundles, which allow groups of neurons to communicate with one another [7].

C. Meninges

The brain is surrounded by protective layers called the meninges. They are made up of three successive membranes:

a) The most internal of these membranes is the pia mater

b) The intermediate membrane is the arachnoid

c) The most external membrane is the dura mater [8].

D. CSF cerebrospinal fluid

Cerebrospinal fluid, or CSF for short, bathes both the brain and cerebellum. The cerebral venous system absorbs and replenishes this fluid, which has an average amount of 150 ml. The fact that it contains immunological mediators produced from both humoral and cellular sources is responsible

for one of its most vital activities, namely protection against infections; nevertheless, it also serves other purposes. The movement of hormones from one brain region to another.

3.2.4 The Brain at The Cellular Level

The information conveyed by the peripheral receptors, which respond to the environment, are analyzed into their components by the brain, and give rise to perceptions; some of this information is stored in memory. On this basis, the brain commands the coordinated movements of the muscles. This whole process is done thanks to the nerve cells and the connections that exist between them. Despite the simplicity of these basic units, the complexity of behavior [complexity evident in all capacities of perception, memory and action] is the product of the concerted activity of a considerable number of neurons. White matter is formed of fibers, while gray matter is composed of cells. The neuron, the cell, and the fiber all have the same fundamental structural components. In the neurological system, glial cells are simply one type of cell. There are also glial cells, which are important for supplying nourishment and support [9].

3.2.5 Neurons

The brain processes and propagates information, whether it comes from outside or inside the body, thanks to neurons, which are cells capable, among other things, of transmitting an electrical signal [10].

The cells that comprise the glia The supporting cells that surround neurons in the central nervous system are glial cells. They connect blood vessels and transport nutrients essential for the nervous system's metabolism, acting as a form of glue for the neurological system (the Greek word for glue is glie). Glial cells are distinguished from neuronal cells due to their ability to divide and their potential to form malignant tumors. There are two major categories of glial cells [11]:

a) Microglia Contributing to the cleaning procedure. The most prevalent type of cell has an isolated cytoplasmic nucleus (12).

b) Macroglia This collection contains [13] distinct components.

c) Astrocytes are the most abundant type of cell in the brain. They contribute to the metabolic process and the formation of the fundamental components of the nervous system, making them real connective tissue.

d) Oligodendrocytes are more abundant and smaller than astrocytes, the major cell type in the brain. The primary function of these cells is to generate the myelin sheath, which is responsible for shielding the axons. Oligodendrocytes and Schwann sheath cells, located in peripheral nerves, are quite similar.

e) Brain cavities and the major canal of the spinal cord are surrounded and lined by ependymal cells. They possess a free edge resembling a brush. They play a crucial role in processes involving the exchange of cerebrospinal fluid and brain parenchyma.

3.2.6 Cerebral Pathologies and Tumors

A cerebral lesion is a lesion that affects the brain. In general, it is a more or less extensive destruction of nervous tissue leading to a deficit in perception, cognition, sensitivity or motor skills depending on the role that the affected region played in the neurocognitive architecture. After the age of twenty, human beings lose thousands of neurons every day. This cellular degeneration is due to a number of brain diseases such as brain tumors. In our end-of-study project, we will focus on the detection of gliomas, which constitute about a third of the most common primary brain tumors.

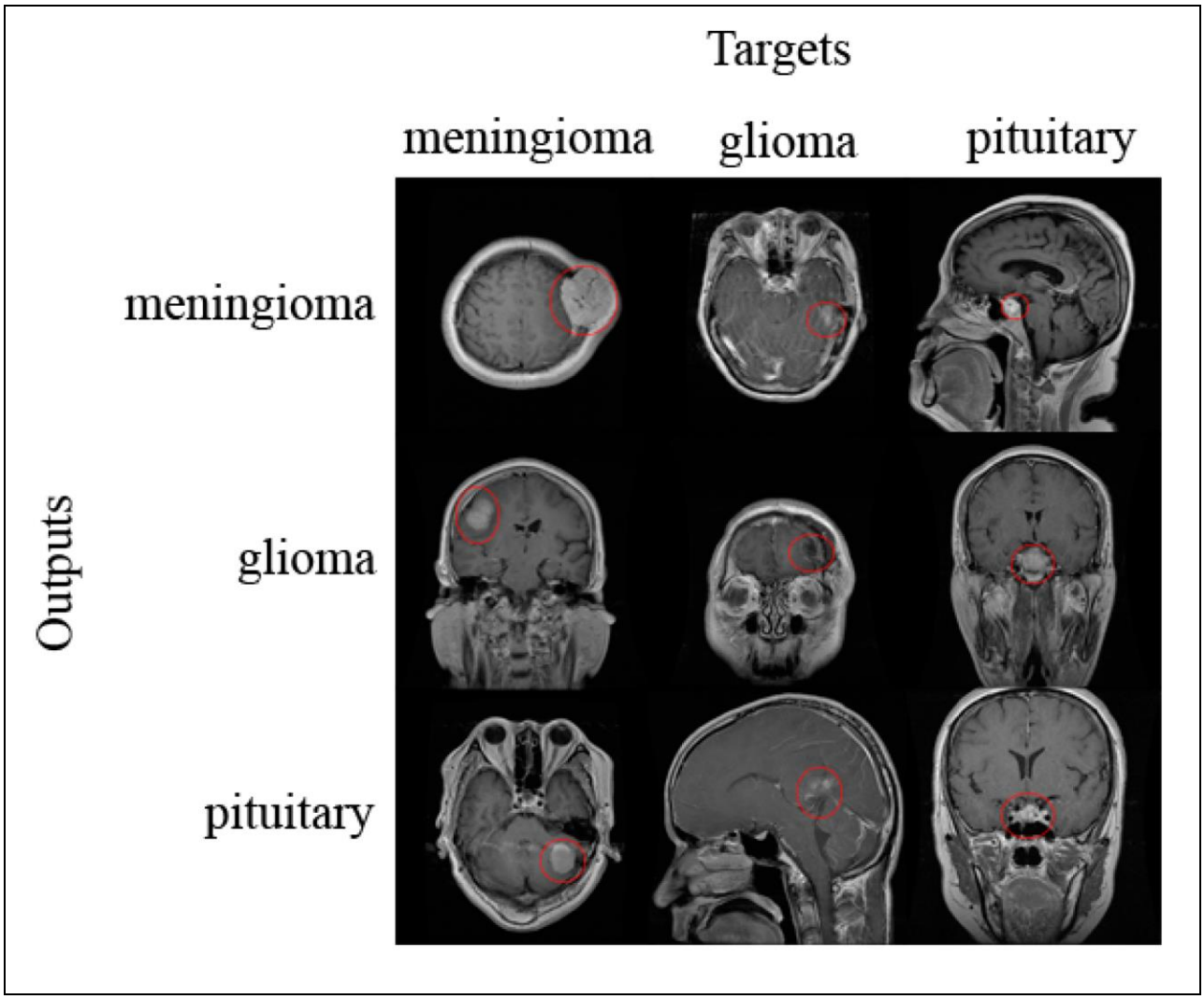

Figure 3.3: Brain Tumor Types in different modalities

A. Glioma

The most prevalent type of tumor that can harm the central nervous system is one that arises from brain glial cells [14]. The neuron is the most important cell type in the brain, and these cells are critical to its functionality. Our cerebral hemispheres, the largest and most peripheral areas of our brains, are responsible for a vast array of functions, including movement, speech, cognitive function, and emotional expression. In addition to respiration, blood pressure, heart rate, optic nerves, and the cerebellum (which regulates balance), there are more processes that can be impacted by the drugs. Among these include breathing, blood pressure, heart rate, optic nerves, and the cerebellum. They might or might not represent a health risk to humans. Gliomas are often

categorized into one of four classifications based on their severity. According to the conclusions of a new study, fourth-grade pupils are the rudest [15]:

a) Astrocytoma.

b) Ependymoma.

c) Glioblastoma.

d) Oligodendroglioma [16].

B. Symptoms Patients diagnosed with gliomas report headaches more frequently than any other initial sign of illness. It is believed that the growth of the tumor, which affects nearby tissues in a cascade-like manner, is the underlying cause of severe headaches. The formation of edema is caused by the pressure placed on the microvasculature by the mass effect. Depending on the location of the tumor inside the brain, the mass effect may elicit symptoms indicative of a brain tumor. For example, tumors originating in the frontal lobe of the brain are known to cause behavioral disorders, whereas tumors originating in the temporal lobe are known to create difficulties with receptive speech. In addition to nausea and vertigo, other symptoms that could be caused by a mass impact include vision abnormalities. Seizures, which account for the great majority of epilepsy cases, are one of the characteristic signs and symptoms of the disorder. The irritation of the cerebral cortex of the brain induced by tumors causes convulsions, which may be focal or generalized in nature. Gliomas can cause a range of symptoms, including tingling sensations, weakness, and trouble walking. In exceedingly rare situations, the tumor may bleed, resulting in an acute hernia syndrome that might eventually be fatal to the patient [14].

C. Risk factors Like most primary brain tumours, the exact cause of gliomas is unknown. But certain factors can increase the risk of developing a brain tumour. Among these risk factors [16].:

a) Age.

b) Exposure to radiation.

c) Family history of glioma

3.3 COMPUTER VISION SYSTEM

Computer navigation systems in the medical field offer new possibilities to experts during surgery to have a better visualization of the anatomical structure and to acquire quantitative information in real time. During a discectomy, the surgeon is required to reduce a certain amount of disc tissue depending on the degree of deformity and it would be important to have real-time quantitative information on IVDs and CVs such as the percentage of tissue remaining, size, position and orientation of the two structures ... etc [17]. In this context, 3D reconstruction of the spine is an excellent means of visualization. The practice of minimally invasive surgeries poses challenges for the development of supportive systems. The incisions made are very small compared to a totally invasive approach. Often, the surgeon can only pass a single endoscopic camera that does not allow full visualization. Also, in orthopedics, metal objects [screws and rods] are often required but further limit access to anatomical structures [18]. Therefore, 3D visualization helps to maximize the chances of success by limiting human error. In the case of scoliosis treatment, with regard to the anatomical structures on which the surgeon focuses, a surgical navigation system must acquire a preoperative 3D model to obtain this 3D model, it is essential to first extract the structures of interest and delimit their outlines in the image, which amounts to the segmentation. An automatic, fast, exact and precise segmentation method therefore plays a very important role in the quality of the navigation system. In this context, MRI is a method of choice for obtaining the information necessary for the reconstruction of the preoperative 3D model. Due to the posture of the spine when taking the MRI which is not similar to that while lying on the operating table, an X-ray of the spine is acquired just before the start of the discectomy. and readjusted on the preoperative 3D model. During the operation, this same model will update in real time using the images that come from the endoscopic camera thanks to a 3D / 2D registration to obtain a visualization of the spine during the surgery.

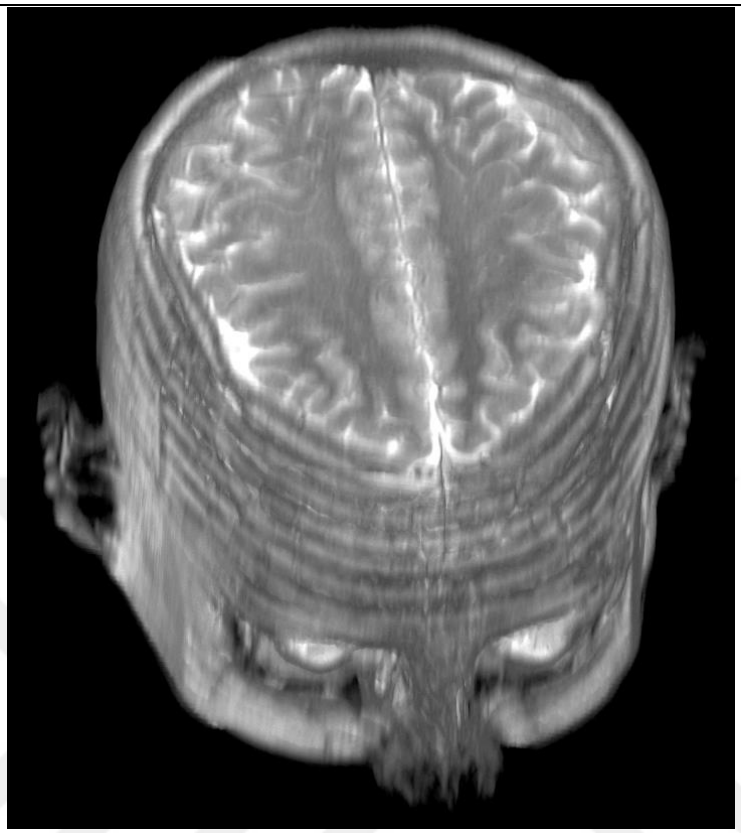

Figure 3.4: 3D MRIs of the human brain

3.3.1 Magnetic Reasoning Images MRIs

[20] Magnetic resonance imaging (commonly known as MRI) is one of the most advanced and widely utilized methods for visualizing brain malignancies. This is due to the fact that the technology does not require invasive operations and has high anatomical resolution. This is owing to the fact that MRI can distinguish between different types of tissues and is easy for patients to endure. In recent years, magnetic resonance imaging (MRI) has emerged as an indispensable technique for the early detection, monitoring, and diagnosis of malignancies. [22] A diagnosis based solely on human intelligence is difficult, time-consuming, and error-prone due to the likelihood of misconceptions, information loss, and visual fatigue. This is the case despite the extensive degree of detail provided by RM. Poor quality, low contrast, or images including artifacts are difficult for the human eye to acclimatize to. All of these characteristics make it more difficult to view the image. [23] In the majority of instances, the borders of the tumor mass are segmented with the aid of a tumor manual, which can only detect considerable tumor movement. [24] A

number of radiologists will need to invest a considerable quantity of time and effort in order to complete the aforementioned in-depth study. Consequently, computer-aided diagnostics (also known as CAD) have been developed to detect and/or evaluate abnormalities in medical imaging, as well as to assist medical assistants with diagnostic precision and neurosurgical procedures. Image analysis and processing are applied to enhance physicians' analytic skills and reduce the amount of time required for proper assessment, therapy planning, and monitoring the evolution of tumor growth.

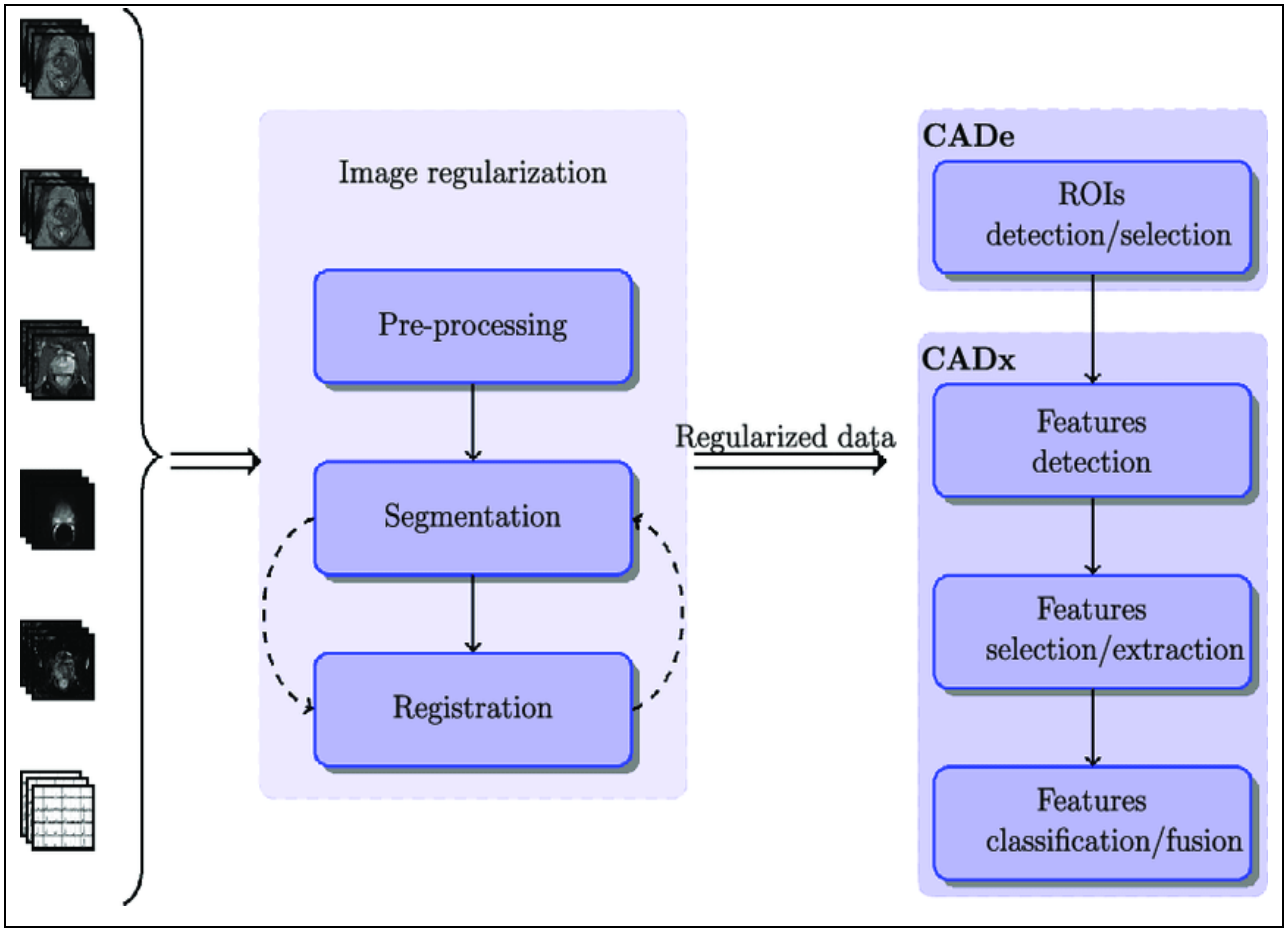

Figure 3.5: Computer Aided detection CAD in MRIs

Radiologists can employ these techniques to obtain a second opinion on medical images, thereby improving the diagnostic precision of their job. [28] Although significant progress has been made in the field of CAD systems, there are still a number of obstacles to overcome in order to increase the sensitivity of these systems. During the process of doing an autonomous analysis of medical images, image difficulties such as noise, which can affect pixel intensity and non-uniformity of

image intensity, must be considered. [29] Consequently, it is required to undertake a thorough examination of various algorithms for all phases of the CAD system's processing, beginning with the pre-processing phase and continuing through the final classification step. This analysis should employ whatever technique is necessary to shorten the processing time for RM. This study employed mathematical, logical, and morphological processes in the T1c, T2, and FSPGR T1c sequences to develop a fresh new method for the automatic mechanics of brain tumors in MRI. The algorithm was developed as part of this research. At the conclusion of the inquiry, the algorithm accurately segmented the tumor region in line with the radiologists' manual.

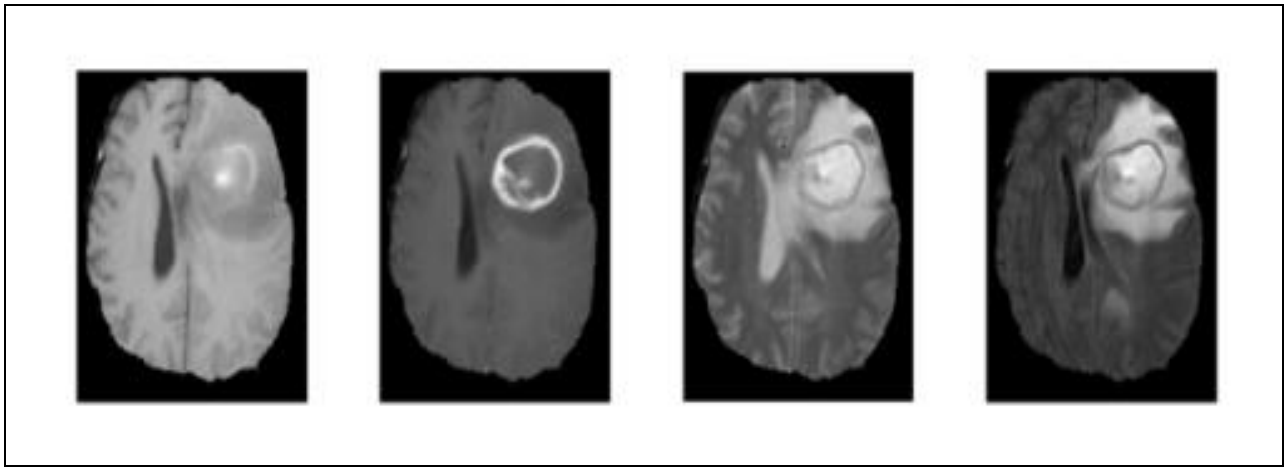

Figure 3.6: Example of Brain Tumors in different modalities

MRI is a medical imaging modality used most often for diagnostic purposes. It does not expose the patient to harmful radiation such as a CT scan. The patient is placed in a strong magnetic field which will stimulate the hydrogen nuclei found in the water molecules of the human body and orient their own magnetizations [or spins] in the same direction. Then, electro-magnetic pulses called radiofrequency waves are emitted and released in order to deflect the spins from their alignment to generate a magnetic resonance signal that will be picked up by the device. Thanks to image reconstruction algorithms, it is then possible to form 3D images representing the specific properties of tissues in relation to these electromagnetic stimuli. MRI is often used in the planning of surgeries as well as in several clinical studies in the study of scoliosis. For example, [31] studied and compared the abnormal differential growth of the anterior and posterior components of the thoracic vertebrae in patients with scoliosis. [33] used MRI to study the degree of torsion of the vertebrae in patients with scoliosis.

3.4 BRAIN TUMORS MRI DATASET

The FLAIR and T1 MRI sequences used in this study originated from the BRATS 2018 Dataset. This dataset contained photos of five distinct individuals collected over the span of four to five days. In order to capture images, a Philips 3T system was deployed. The T1 sequence had a TE value of 6 milliseconds and a TR value of 10.3 milliseconds. The FLAIR sequence had a TE value of 68 milliseconds and a TR value of 11,000 milliseconds. Without these, the T1 sequence could not have been achieved. In 2016, 15 persons were photographed for the MICCAI database using the GE Discovery 3T, Siemens Aera 1.5T, and Siemens Verio 3T cameras. These photographs were obtained at the Hospital das Clnicas de Botucatu in Brazil utilizing Siemens' 3T technology. The T1 sequences were obtained with a time resolution of 465 and a time element of 9 milliseconds. The FLAIR sequences had a TE of 80 microseconds and a TR of 9,000 milliseconds. Then, 3T Siemens Magnetom Trio pictures were retrieved from a database maintained by the University of Ljubljana. The T1 pictures were acquired by setting the time constant (TE) to 20 milliseconds and the repetition time (TR) to 2000, whereas the FLAIR images were acquired by setting the time constant (TE) to 392 milliseconds and the repetition time (TR) to 1000. (TR).

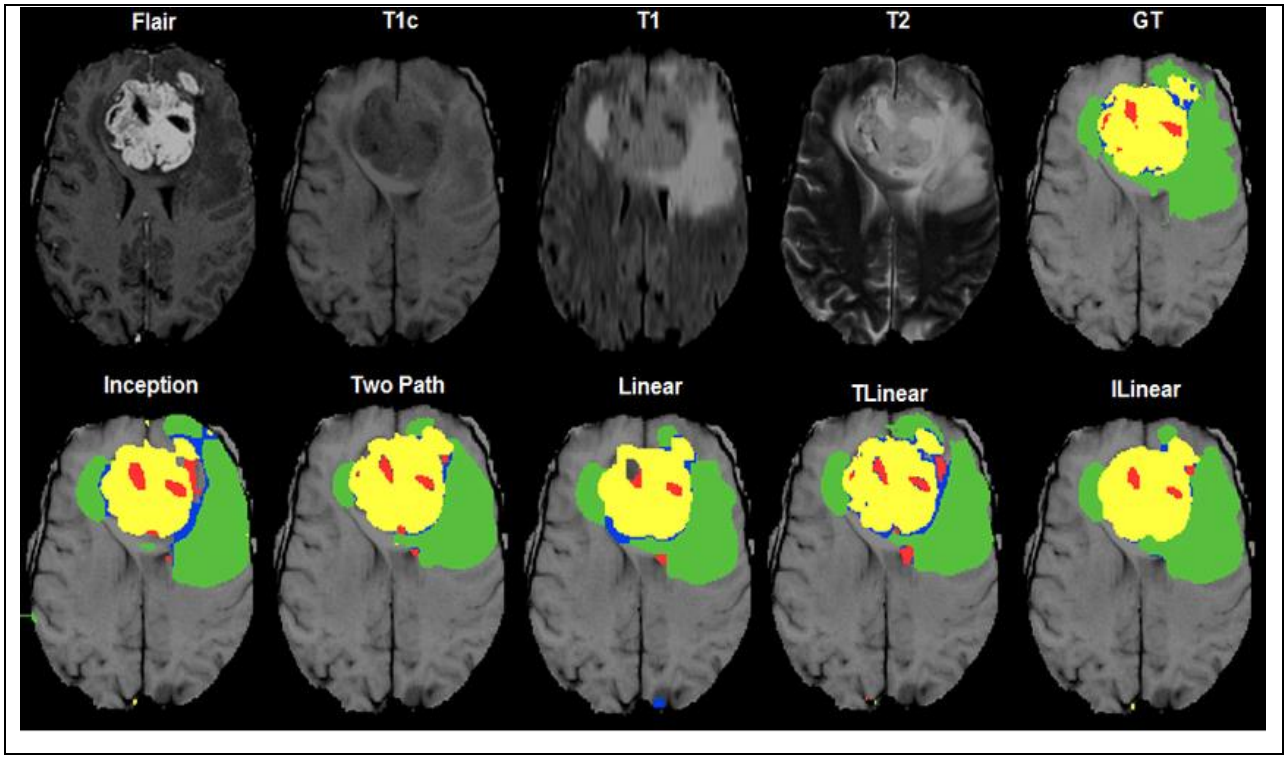

Figure 3.7: Brats dataset

3.5 DEEP LEARNING

Machine learning is a field of artificial intelligence whose objective is to train models to solve one or more problems from a set of so-called learning data presented in the form of examples. Learning can take place unsupervised, supervised, or sometimes a combination of the two [38]. We speak of supervised learning when an example represents a pair of data xi and its label yi. The goal is to train a model to learn a prediction function from a set of observations representative enough to allow it to predict the real label of unobserved test data belonging to the same population. We talk about solving a regression problem if the goal is to estimate a continuous value or classification if the set of output values is finite. For example, in this thesis, the segmentation problem can be considered as a supervised classification because we have three classes [Background [AP], CV, DIV] and a voxel of an image can only belong to one between them. A classifier is evaluated by its ability to correctly predict that a piece of data xi is associated with its class y but above all to generalize its solution to the entire population. The generalization is estimated by the bias and the variance of the classifier. Bias is defined by the difference between the average prediction made by the classifier on the validation data and the actual value. The variance is defined by the sensitivity of the classifier to fluctuations and to vary its prediction for an observation during training. High variance means a model that is unable to find a real relationship between the data. At best, a well-trained classifier has a low bias-variance ratio, so we could speak of a model that generalizes well. As part of our project, the ideal scenario would be to train a classifier that is able to recognize IVDs and CVs accurately regardless of the MRI modality and regardless of the degree of severity of scoliosis. However, classifiers are subject to two phenomena to be avoided: over-learning and under-learning. The first is characterized by the inability to perform well in the face of data not observed during training. In this case, the bias is therefore high [39]. As for under-learning, it is simply the inability of the classifier to pinpoint the learning data. In this case, it is the variance that is high. This can be manifested by a lack of data for training or by a complex classifier. This is linked to the number of parameters it contains. Machine learning comes in a variety of algorithms. These algorithms are located on a spectrum whose extremes correspond to two categories: parametric and nonparametric. Parametric algorithms are more traditional.

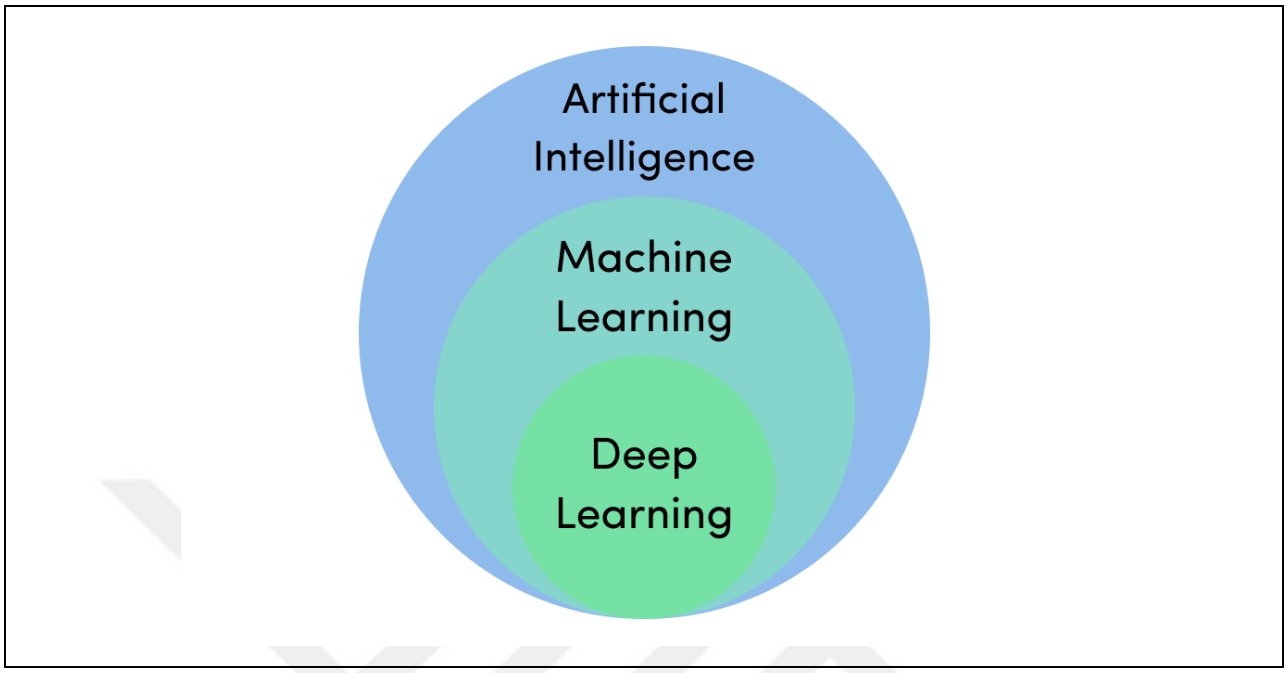

Figure 3.8: Deep Learning position in the AI hierarchy

Two of the most well-known methods in this category are Support Vector Machines [SVMs] and perceptron. These algorithms are known to be limited in their learning capacity because the number of parameters must be determined manually beforehand. The non-parametric methods are more sophisticated. The number of parameters adapts to the number of training data. The more it increases, the more the capacity of the model also increases. Theoretically, the number of parameters can go up to infinity. This gives these methods greater flexibility and allows them to result in models which have a better scope for generalization. Our project is devoted to probabilistic statistical learning, more particularly to neural networks in their non-parametric version. The goal of statistical-probabilistic learning algorithms is to model the distribution of classes Y conditioned on the data X. We denote this distribution p [yi | xi; w] where w corresponds to the parameters of the model. Concretely, the algorithm aims to maximize the expectation of the output distribution of the model pmodele [y | x; w] on the set of training data X and their labeling Y. It is an iterative process which aims to maximize the likelihood of the training data. This maximization amounts to describing an objective function J on these data [Goodfellow et al., 2016]. We notice:

$$J[w] = E_{X,Y \sim P_{donnes}} L[X, Y, w] \qquad (3.1)$$

The cost function L is used to determine the rate of prediction error that the model achieves on the training data. w is the vector of the parameters. The learning process tends to minimize error by adjusting the parameters:

$$w^* = \underset{w}{\operatorname{argmin}} J[w] \qquad (3.2)$$

Optimizing the parameters of a model can be done in several ways. In machine learning, the most popular method is the gradient descent algorithm introduced by [40] It is an iterative process which calculates at time t the gradient of the function J with respect to the vector of parameters wt and advances in its opposite direction until reaching a minimum but without guarantee that it is global: where f [x] is the prediction of the model, Δ is the derivative of the function f which informs about the direction and the amplitude of its gradient. In the development presented so far, there is no indication of the distance to be covered. To do this, a hyperparameter is introduced as the gradient descends which will represent the learning rate α per iteration. The calculation of the new vector of parameters is therefore done like this: In reality, the choice of α is crucial. This determines the speed of convergence. Too large a value leads to too abrupt changes where the gradient goes from convergence to divergence without reaching optima. Too small a value theoretically allows an optimum to be reached but would take a significant amount of time. The gradient descent algorithm has inspired several optimization methods.

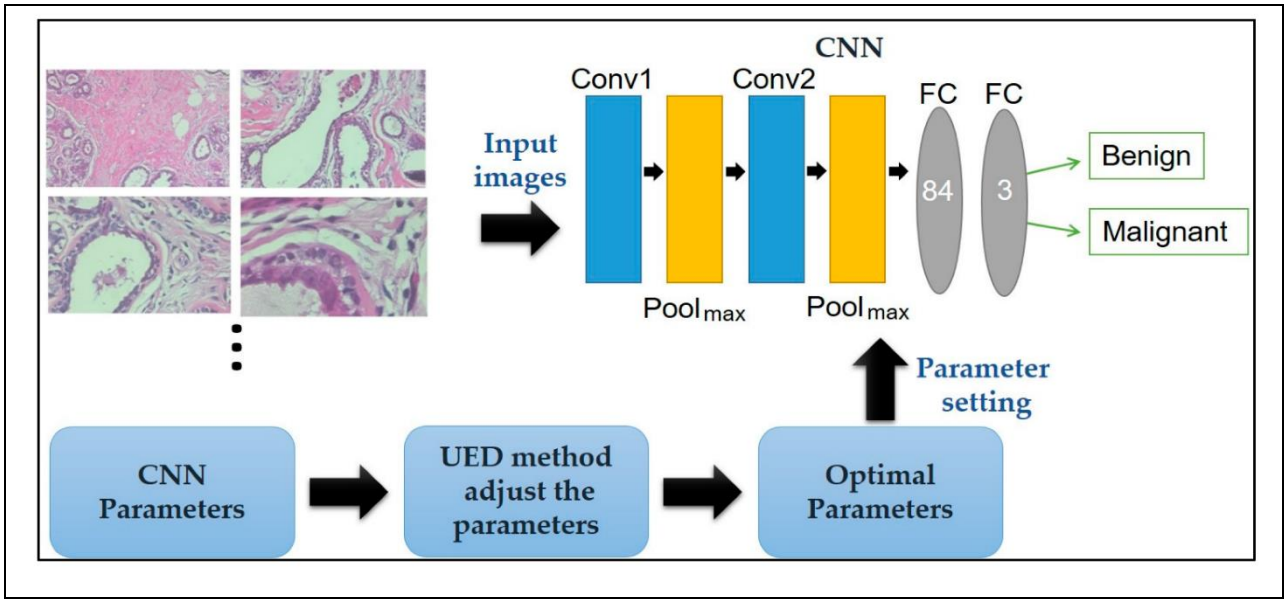

Figure 3.9: Deep learning feature optimization

From a practical standpoint, its simplistic version is very limited. This is only applied after passing all of the training data to the model, which leads to a single gradient calculation per iteration. Training is therefore very slow, if not impossible if all the data cannot be retained in memory. The stochastic gradient descent algorithm worked around this by optimizing the parameters after training each example. Convergence is thus faster and makes it possible to explore other regions in the hope of finding a better local optimum. However, convergence towards the global minimum becomes more complicated. The mini-batch gradient descent algorithm has been proposed to benefit from the advantages of the two previously mentioned approaches by performing the optimization after training on n training data. However, the descent of the gradient by mini-batch does not solve all the limitations. The choice of the learning rate remains empirical and a single value may not be suitable for all stages of parameter optimization where the behavior of the gradient in the hollow areas remains unpredictable. One thus notice oscillations of the parameters without effective convergence which tend towards a stagnation. To reduce this problem, the momentum [43] is introduced in the algorithms of the descent of the gradient, which allows the model to keep a history of the previous directions of the gradient. The momentum improves the quality of the optimization because the calculation of the derivative of the cost function is not entirely accurate. It is rather estimated on a batch of data. The direction of the gradient is therefore not optimal. Adding a term that indicates the calculation of the derivative on the old decisions allows a better estimate. The evolution of machine learning has led to models with very large capacity but difficult to train. Numerous studies have therefore focused on better guided optimization, in particular thanks to the adaptive learning rate. Logically, the latter should increase when the gradient is large which means that it takes the direction towards an optimum zone and vice versa in the opposite case to avoid the divergence. With this in mind, Kingma & Ba [2015] proposed Adam, an optimization algorithm that is of particular interest to us because it is the one we use in our project. Adam estimates a different learning rate αi for each parameter wi by estimating the mean and variance of the previous gradients. The authors also proposed a way to limit the influence of the first derivatives calculated during the first iterations.

3.5.1 Artificial Neural Networks

Many years ago, processors surpassed the human brain to solve complex calculations in record time that keep getting shorter. However, the innate perception of humans is extremely difficult to reproduce digitally. Neural networks are models that are inspired by the functioning of the human brain to achieve a processor with such a perception. A biological neuron [Figure 1.5] consists of a cell body with a nucleus and extensions called dendrites, a nerve fiber called an axon, and a synaptic area made up of synapses. A neuron generates an electrical signal and transmits it to another neuron via synapses. If the signal is stimulating enough, the dendrites of the receptor nucleus will activate to receive it and relay it in the same way to another neuron by making it travel its axon. Artificial neurons [Figure 1.6] are connected to each other and transmit information to each other in the same way. The output of a neuron is just the weighted sum of its inputs. An activation function is applied to this output to estimate whether the signal is stimulating enough and needs to be propagated. Mathematically the output of an artificial neuron is:

$$y = f\left(\sum_{i}^{N} x_i \cdot w_i + b\right) \qquad (3.3)$$

where xi is a digital data input to the network weighted by the associated weight wi. b is a term called bias whose role is to translate the activation function f. The artificial neuron alone is of little use. On the other hand, the idea gave rise to machine learning and a large panoply of algorithms have been developed with the idea of going from a neuron to a neural network. This is illustrated in the family of parametric statistical learning algorithms.

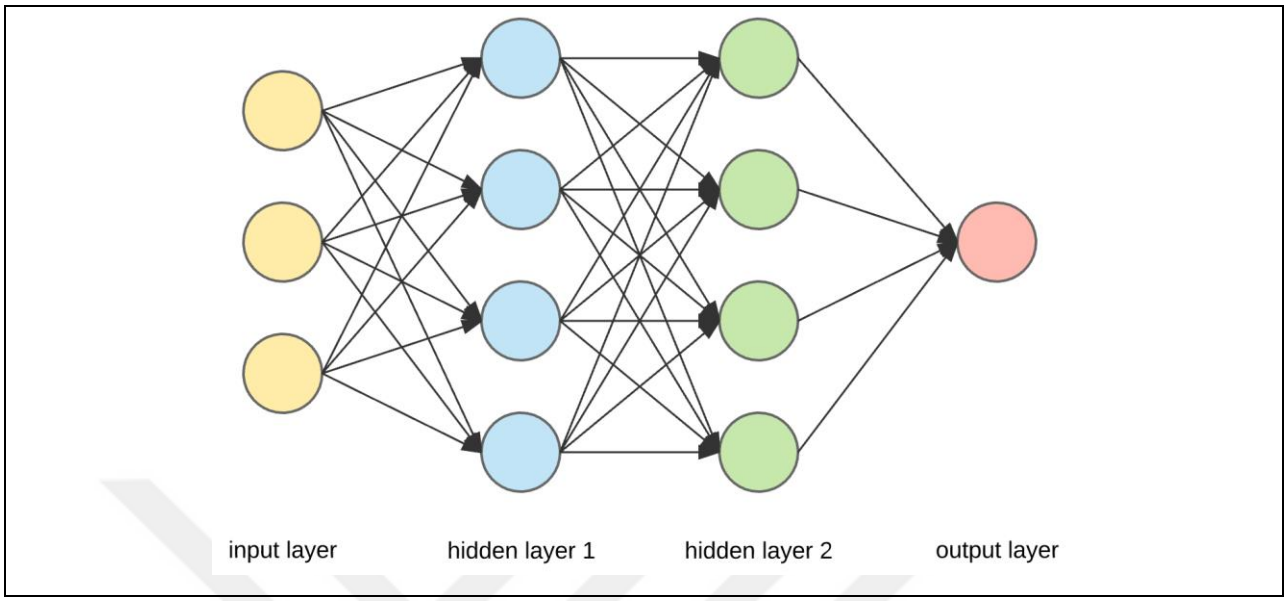

Figure 3.10: ANN Structure

We can mathematically define the neural network as a function f parameterized by weights w such that: fw [x] = y. It is composed of an input data layer connected to a hidden layer which contains a number of neurons which in turn is connected to an output layer. This evolved into a Multi-Layer Perceptron [MLP]. We can express it as a succession of nonlinear functions cascaded where gwj [xj] corresponds to the I layer hidden. We can also see a neural network as an extractor of features which are only the results of the transformations undergone by the data in x inputs. However, the more hidden layers a neural network has, the more parameters there are to optimize and the more difficult the training. Neural networks were just endowed with greater capacity than their predecessors, but without knowledge of how to train them effectively. We had to wait for better processors but especially the backpropagation algorithm proposed by Rumelhart et al. [1988], an elegant way to propagate the cost function [Equation 1.1] over the set of weights and optimize them so that neural networks can reveal their potential. Research by [44] demonstrated the ability of a neural network to solve any continuous function in a closed space provided that the model is endowed with a large capacity. This comes down to one of their properties which allows them to extract characteristics on their own and paves the way for their use in various fields of application. In image processing, [45] introduced what interests us particularly in our work: a first convolutional neural network [CNN] whose architecture was called LeNet5, an algorithm allowing classifier with high precision of handwritten digit images. Subsequently, the advances made by [46] have made it possible to effectively train deep neural networks where several hidden layers

follow one another forming a non-linear representation whose complexity increases as one goes deeper.

3.5.2 Convolutional Neural Networks

Reconnectors of consumers are patterned after the cerebral crust, a portion of the brain that processes sensory information, in their most basic form. Figure 3.11 depicts an example of a common network topology. This structure is composed of layers of nodes, each of which activates in response to a specific type of input. Through weighted connections, the consequences of these activations are relayed to the vehicle nodes. After the data has traversed all levels of nodes and connections, some sort of output is subsequently transferred outside the red. The ability to fine-tune the weights of the connections between the nodes in order to increase the accuracy of the answers they generate is what makes neural networks so successful and advantageous for handling such a wide variety of data-controlled problems. We are particularly interested in the Convolutional Neural Network variety of neural network. In addition to an entering cover, a disguised cover, and an exit cover, the standard NN also provides an exit cover, however these CNNs provide a fourth form of cover that has been shown to be particularly useful for learning knowledge about images. They adhere to many of the same ideas as regular NN. In this example, the red entries will represent the output segmentation labels from a magnetic resonance picture.

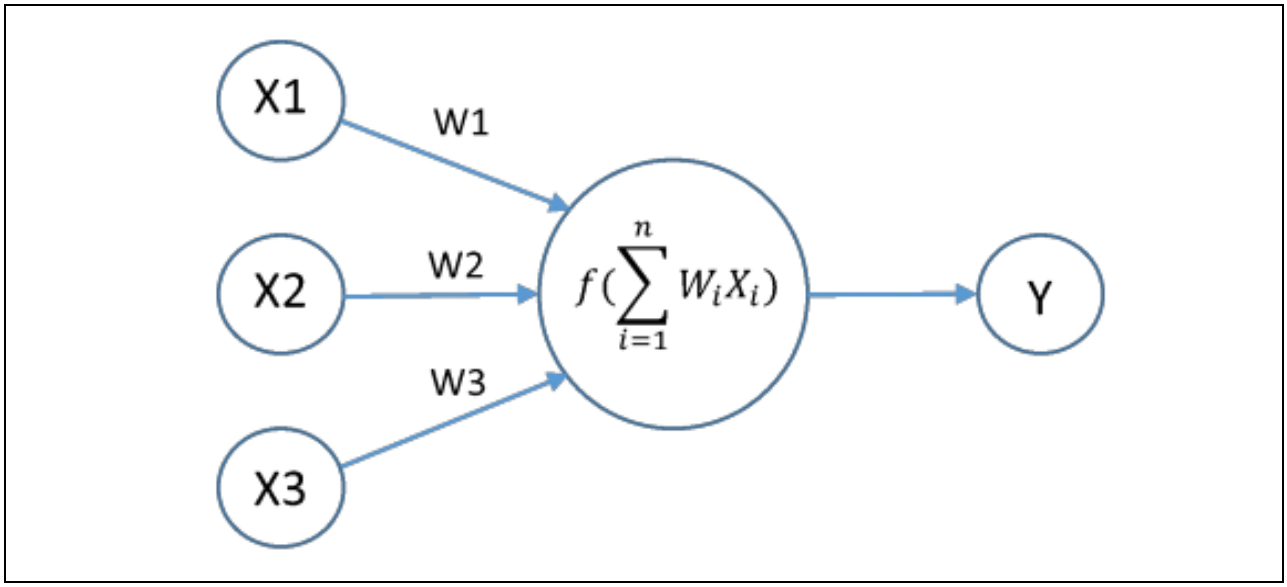

Figure 3.11: Artificial Neuron

CNN is distinguished from other neural networks by its initial convolutional layer, despite the fact that other neural networks also contain convolutional layers. In addition to compressing the data into bits of recognized data, these covers are also used to indicate items of interest. This layer applies a convolutional modification to a series of values representing the pixels or voxels of an input image patch. The previous layer can supply these values. CNN employs a filter known as an interchangeable filter, neurons the kernel, which is another matrix that encodes a characteristic, and in many cases the random kernel. The receptive field is covered by this kernel, which is located in the upper left corner of the entry. After multiplying each element separately, the receptive field matrix is multiplied with the kernel. In the same relative position as before, the summaries of the outcomes of the multiplications are preserved in the feature map immediately following the location where those results were recorded. Now that the kernel has been maximally twisted, we have a feature map that is full and ready for use as input. Convolutions that occur between the kernel and the input are displayed on the matrix-shaped feature map. Utilizing these feature maps as a starting point for the design of future covers is possible. To describe this idea in a different manner, we could say that a convolution is a function action. Images can be deconstructed into two independent functions: one that processes incoming data and generates a position within the image, and the kernel, which works as a filter. Obtaining an output is achievable throughout the process of computing the product of points between the functions. To advance to the next image location, the filter will move to a new position. This new location will depend on the distance of each step. The calculation must be performed an unlimited number of times until the entire image has been processed in order to build a feature map. Depending on its current location, the kernel can be viewed and defined on this map as either a straight line, a point, or a curved edge. When a facial image is fed into a CNN, the filters are responsible for identifying features like as lines and edges. Eventually, these feature maps will converge into entries for the next layer of CNN architecture, just as feature maps will converge into one another.

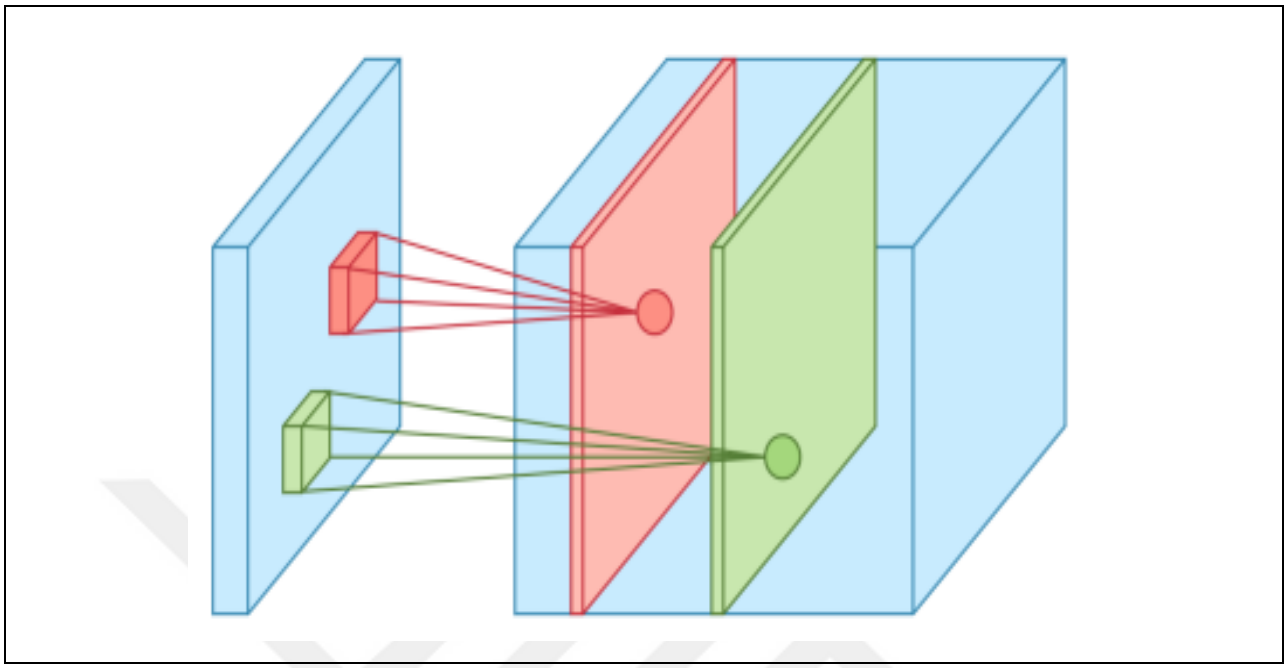

Figure 3.12: Convolution Process in Artificial neural network

4. PROPOSED METHOD

4.1 U-NET

The U-Net network, which was established in [36], greatly simplifies the segmentation of medical images. In order to retain the image's proportions, a series of convolution, pooling, and deconvolution layers of equal length are used. As soon as the input has been reduced to its most manageable size, it starts monitoring the input's most significant characteristics. The last step is to deconvolve these attributes before combining them with the other attributes belonging to the same dimension. Figure 4.1 depicts the configuration supplied to U-Net. Categorization networks must have access to more than simply the global meanings of the deeper attributes for accurate pixel classification. After concatenating the outputs of the shallow layers, the information is gathered in a relatively tiny region. Contrary to skip connections, these components are concatenations, which significantly differentiates them from skip connections. The diagram labeled Figure 4.2 is an excellent starting point. Using the U-foundation, shape's it is possible to transmit a vast number of information about a subject. When data from the encoder's fundamental features are merged with information from the surrounding surroundings, more complicated features result. The encoder identifies the complex global properties first, and then the decoder utilizes the encoder's knowledge to identify the complicated global properties locally. Due to the fact that the decoder's 120 features were gathered using the same spatial dimensions as the input, each pixel now contains 120 distinct properties. The suggested method for detecting diseases related with spine tumors is a CNN convolutional neural network-based classification-based deep learning technique. In contrast, procedures for identifying and segmenting spinal hemangioma tumors are necessary.

4.2 IMAGE ACQUISITION AND PRE-PROCESSING

To do any kind of image processing, the initial step is to obtain the picture. A variety of medical imaging procedures may result in the generation of pictures with undesirable background noise. As a result, images generated by imaging techniques such as magnetic resonance, computed tomography, and mammography have an abundance of artifacts and background noise. The tumor location in the input picture may be covered by the noise due to segmental obstructions caused by the noise. In order to remedy this issue, a picture is first pre-processed to remove any undesirable

odd numbers, and only then is it sent on for further processing. It is possible that noise reduction, filtering, picture enhancement, and normalization are included in this pre-processing phase.

4.2.1 Normalization

The technique of attempting to scale data between a maximum and lowest value is known as data normalization, and it is a frequent pre-processing step. potential outcomes (both linear and nonlinear) Figure 4.1 is an excellent example of linear normalizing in practice.

$$x_{\text{normalized}} = (\text{ desiredMax } - \text{ desiredMin }) \frac{(x - \min(x))}{\max(x) - \min(x)} + \text{ desired}$$

$$x_{\text{normalized}} = \frac{\text{desiredMax } - \text{ desiredMin}}{1 + \exp\left(-\frac{x - \beta}{\alpha}\right)} + \text{ desired Min}$$

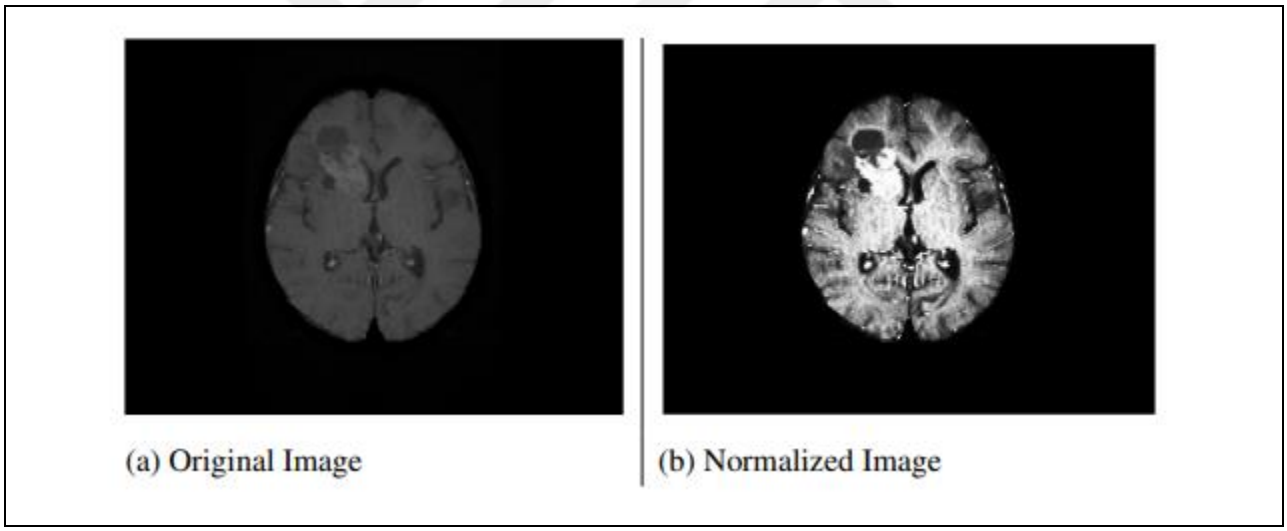

Figure 4.1: Nomadized Image vs non normalized image

4.2.2 Histogram Equalization

The photographs may be normalized by comparing their separate histograms to the histogram of a target picture. This operation may be difficult to do when trying to segment a brain tumor since not every patient has a brain tumor. Even if there is no tumor present in the brain image, the histogram matching method may result in the appearance of certain pixel intensities that are intended to indicate tumor locations. This method improves the image's contrast, resulting in a more consistent histogram. In contrast, this has a significant effect on the data. It is more difficult

to discern between foreground and background items when using this technique. Utilizing a foreground mask will aid in the avoidance of artifacts while dealing with the segmentation of brain tumors. Figure 4.3 is an example of histogram equalization with and without a foreground mask, respectively. Using a mapping function to create the most feasible linear ramp-shaped cumulative distribution function is one of the most common methods for constructing an equalized histogram. Numerous elements must be considered, including the final histogram, the mapping function used to map the pixel intensities in the original image, the image's histogram, and the image after it has been equalized for its histogram quality. All pixels with a value of zero are assigned the value 140 in order to generate an equalized histogram with a nearly linear cumulative distribution function. As a result, the information contained in e is severely compromised.

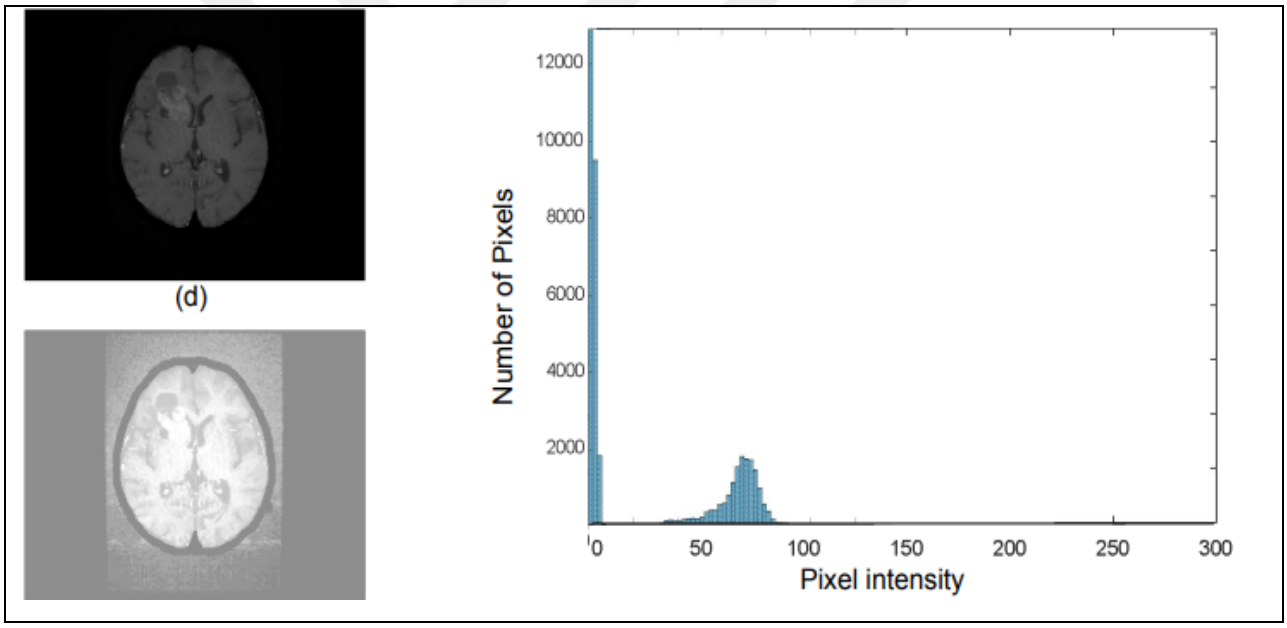

Figure 4.2: Histogram equalization applied w

4.3 SEGMENTATION USING CNN

This is the most crucial and basic step in applications such as the identification of malignancies. It is common practice to divide an image into smaller, more pertinent sections in order to better comprehend what the image depicts. According to the study conducted, there are several methods for dividing a picture. After the segmentation procedure is complete, further processing must be performed to polish the edges and eliminate distracting features. During this process, known as "feature extraction," a photograph's characteristics are extracted for the purpose of analysis.

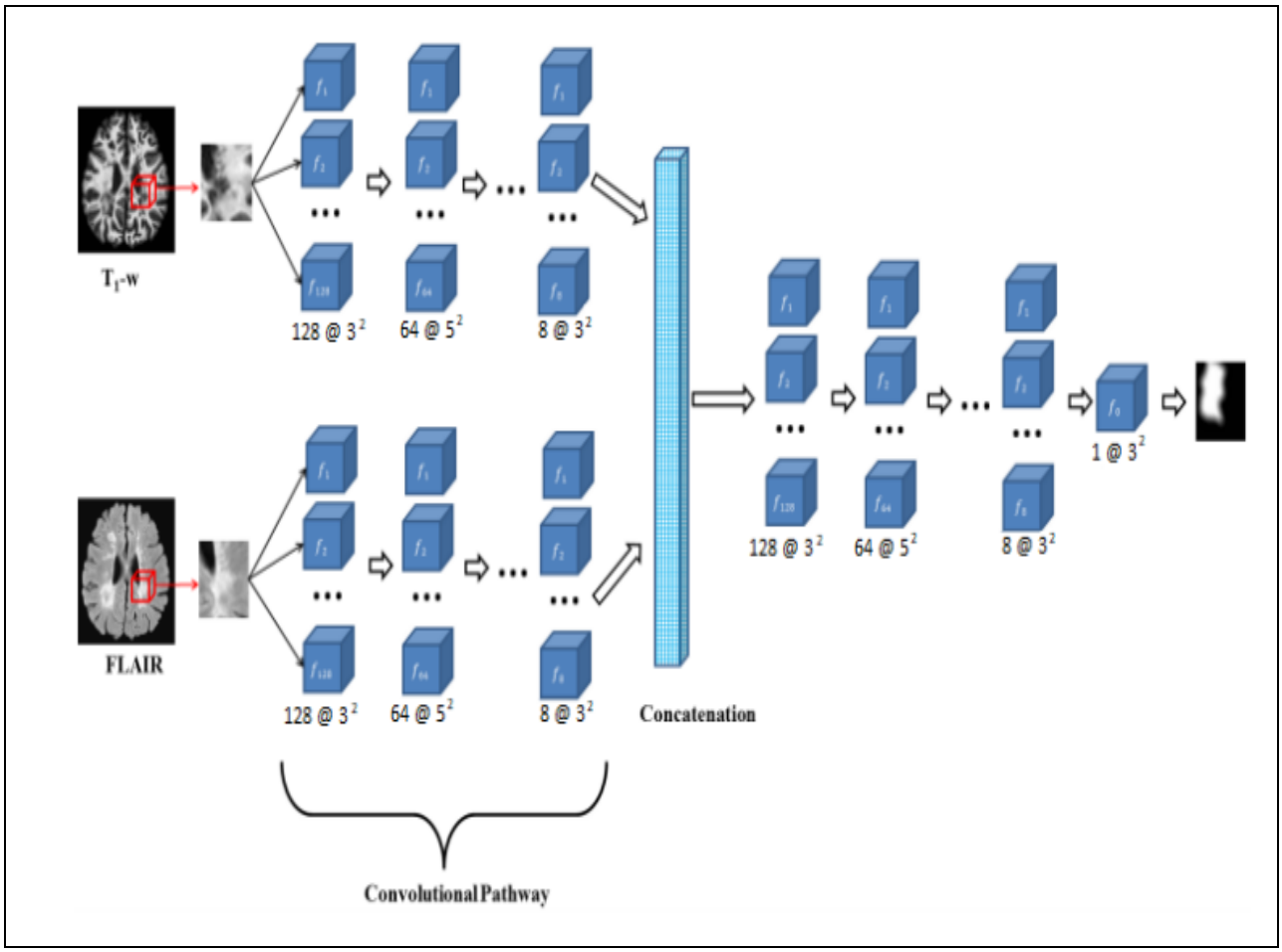

Figure 4.3: Feature Extraction by CNN.

It will be able to forecast the size of the tumor with more precision, allowing a greater number of surgeries to be performed with superior outcomes. Using morphological processes, edge detection methods, or histogram equalization are three methods for effectively extracting undesirable traits. This approach utilizes the link between two identical networks in order to generate a segmentation of medical images. The objective of both networks is to reduce the number of false positives and false negatives within the classifications of the first network. Due of the relatively small amount of voxels in the picture that reflect tissue damage, sufficient voxels are available for training the nets.

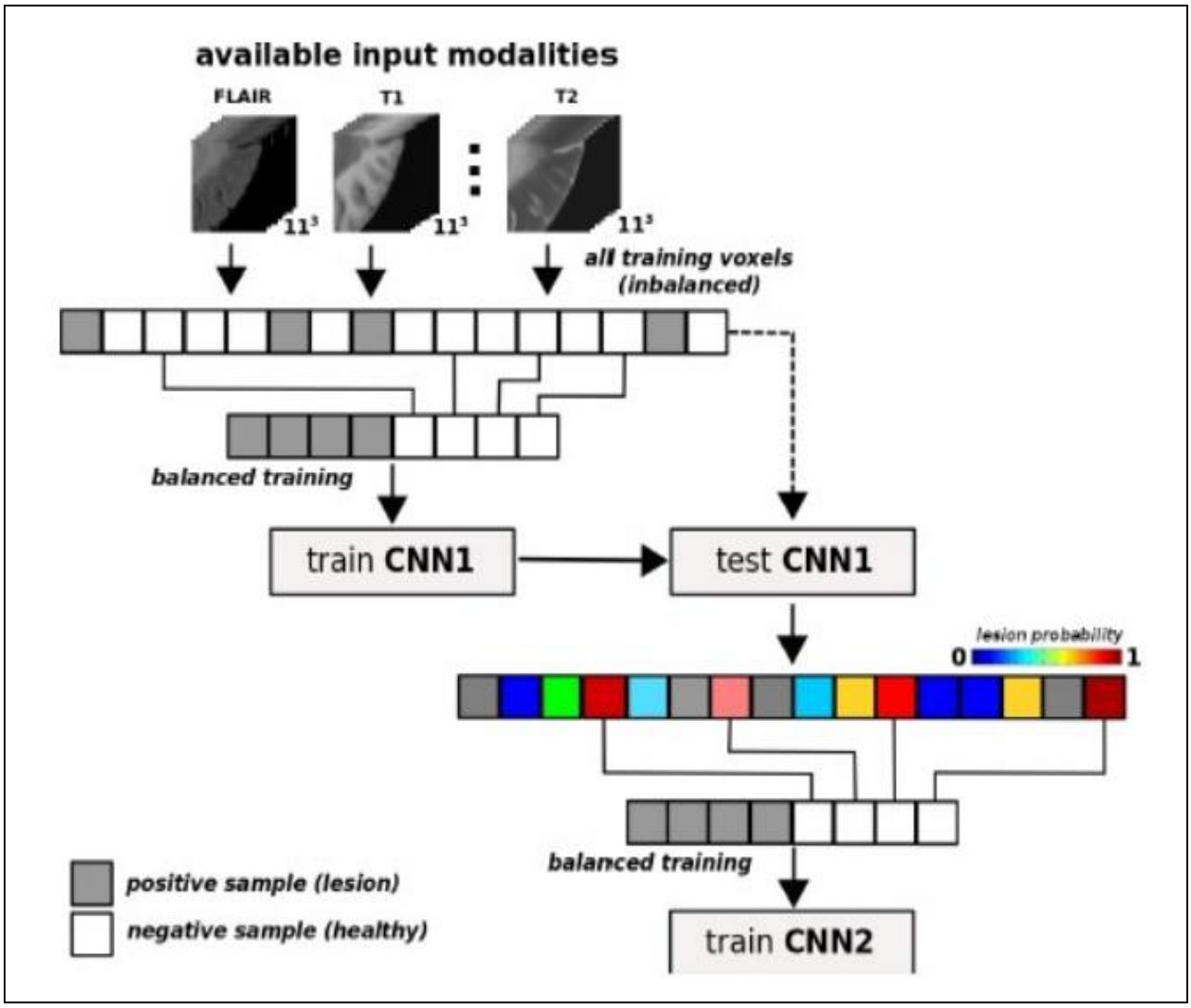

Figure 4.4: Segmentation Using CNN model

The neural network that was shown there was the obvious choice given that Isensee et al. [15] had already demonstrated its effectiveness in segmentation. [Must include bibliographical references] It is based on the encoder-decoder architecture that can be found in various recent studies dealing with the segmentation of medical pictures and won third place in the Brain Tumor Segmentation (BraTS) competition that was organized by MICCAI in 2017. This competition took place in 2017. It was altered such that it could take as input five different three-dimensional patches. These patches were taken from pictures weighted in time 1 (T1W), time 1 with a contrast agent (T1Wc), time 2 (T2W), time 2 in Fluid Attenuated Inversion Recovery (FLAIR), and proton density. This is due to the fact that a radiologist will frequently assess these sequences in order to determine whether or not lesions associated with multiple sclerosis are present (PDW). The first objective of

the unsupervised phase is to make an estimate of the amount of content that can be retrieved from a patch. We are keeping our fingers crossed that the challenge of segmenting brain lesions and this one of multiple-output regression are identical. To finish the first unsupervised target task, it was sufficient to train the encoder component of the segmentation neural network. This is because conducting reconstructions was not required in order to complete the task of regression. The first network was trained to predict the coordinates of the extraction of a three-dimensional material patch (x, y and z). The weights from the trained encoder were moved to the segmentation encoder so that it could be used to segment lesions caused by multiple sclerosis while being supervised. Throughout the course of the program, patches were evaluated and given points. Figure 4.5 depicts the process being followed. We worked with photos that had been standardized.

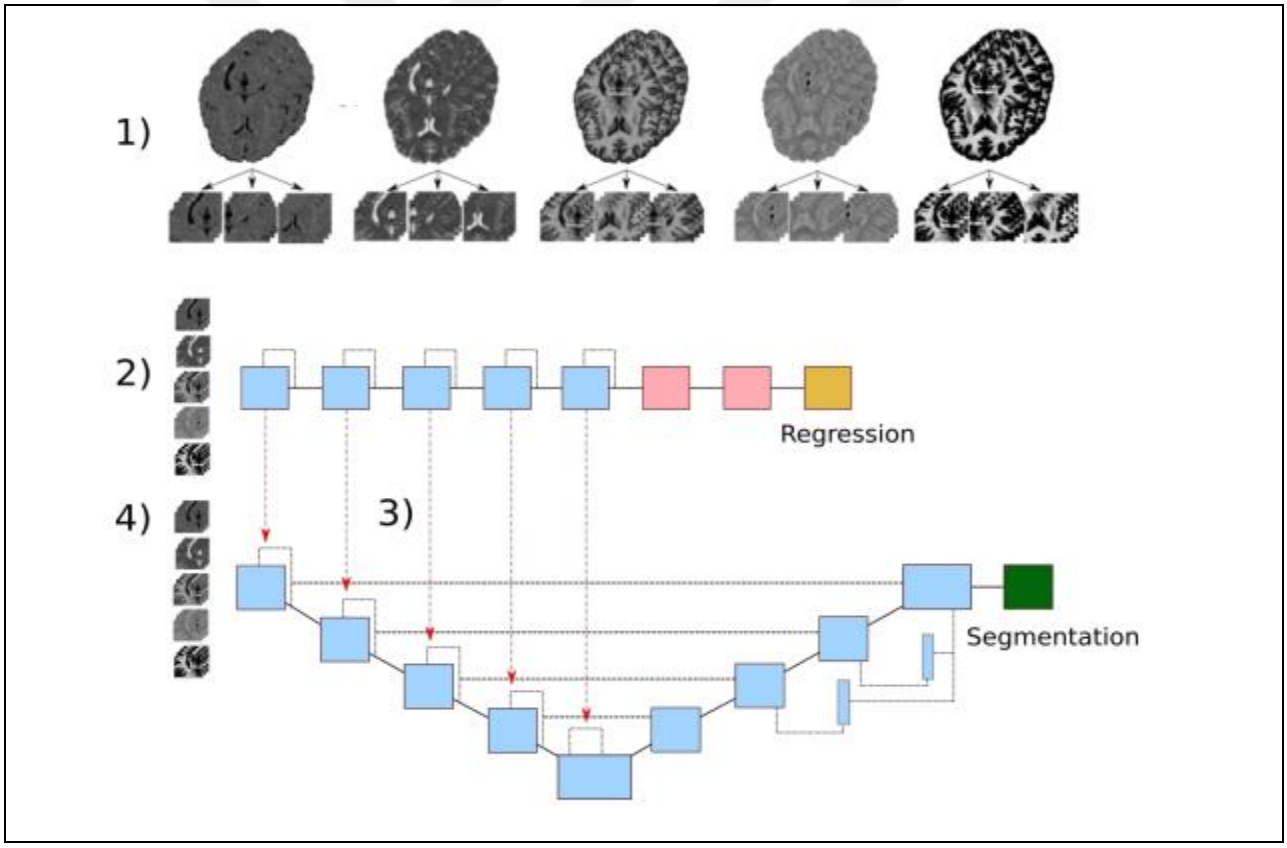

Figure 4.5: Whole System steps summarized

Patches of 32, 32, and 32 voxels were resized to fit within grids of 128 voxels, 128 voxels, and 128 voxels respectively. each other. The optimal size for a patch is one that is both large enough to contain the lesion and the environment immediately surrounding it, as well as small enough to enable the collection of as many subsamples as is practically possible given the available resources

and time constraints. The choice that Roy and his colleagues [31] made has already produced favorable outcomes. Even though including additional data in the training for our CNN might have resulted in improved performance, we decided against doing so because doing so would have dramatically increased the length of our sessions. As an extension of the procedures described in [9] about the dropout sequence, T1Wc and PDW were replaced with "empty volumes" during the training phase. This was done to ensure that the dropout process was carried out correctly. This strategy involves randomly setting the input modalities to zero in order to assess whether or not the CNN adjustment model is sufficiently wide to produce reliable predictions even when the modalities are not there. During the training process, we make use of cross-validation by periodically selecting samples at random from a larger pool. Twelve patches, each containing at least 75% of the patient's brain, are chosen at random from the patient's brain, and all twelve patches come from the same patient. Throughout the course of this treatment, patches that are empty of brain are removed. CNN was given the mission of educating itself in order to improve the accuracy of the Dice score, which determines the degree to which two samples are comparable to one another. As stated in Equation 4 of Figure 2, its computation is a compromise between accuracy and sensitivity 1 in order to limit the influence of an uneven data distribution on the evaluation of the results. This is shown in the figure as "Compromise between accuracy and sensitivity 1." This was done to ensure that the reliability of the findings was maintained at all times. It is possible to utilize the Adam optimizer to cut down on the amount of time needed for convergence [18].

$$\begin{aligned} \text{Sensibilite} &= \frac{VP}{P} \\ \text{Precision} &= \frac{VP}{VP + FP} \\ \text{Dice} &= \frac{2VP}{2VP + FP + FN} \\ \text{Dice} &= 2 \cdot \frac{\text{Precision} \cdot \text{Sensibilite}}{\text{Precision} + \text{Sensibilite}} \end{aligned} \tag{4.1}$$

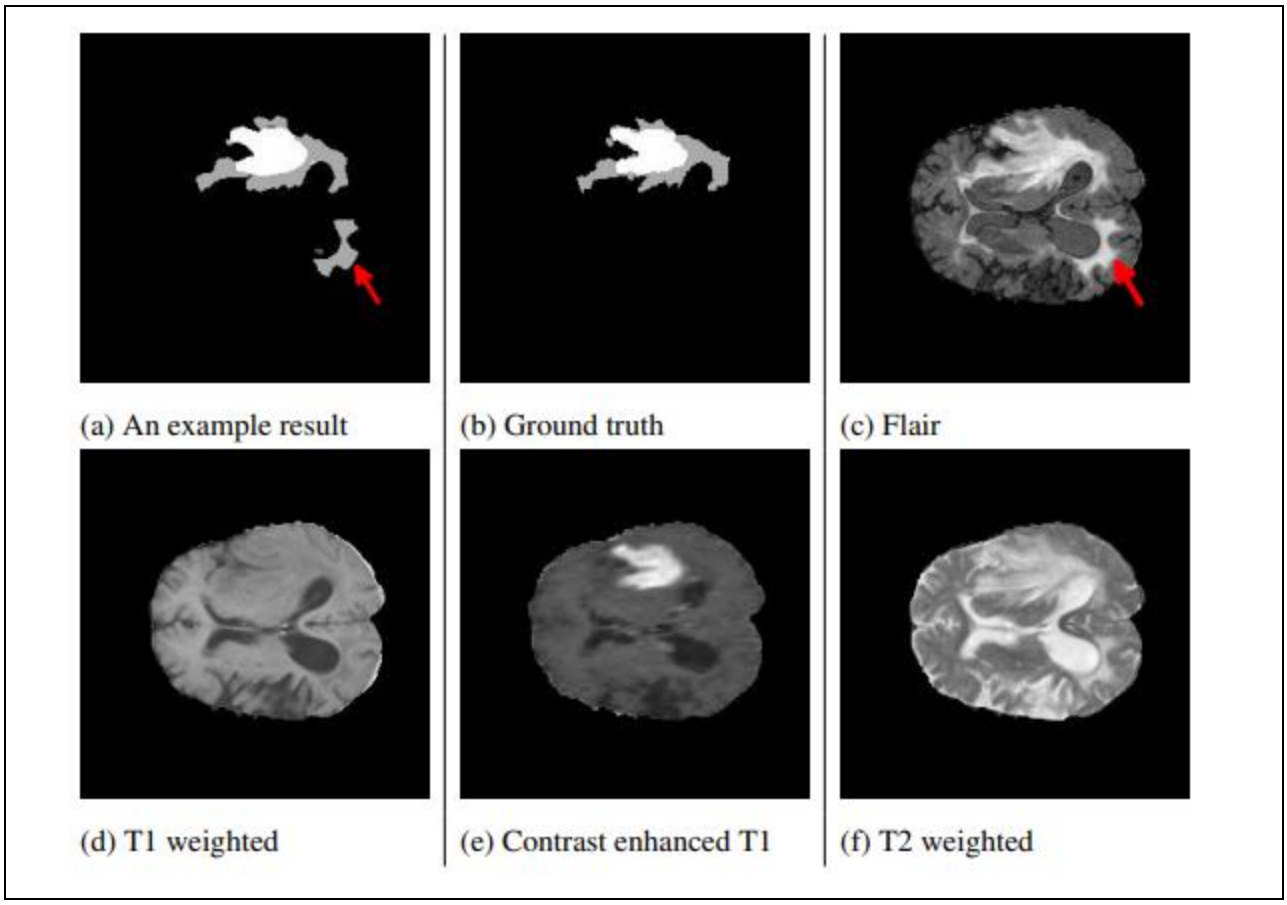

Figure 4.6: An Example result

4.4 CLASSIFICATION OF SEGMENTS

CNN needs to be trained to recognize the tumor before we can even begin to investigate whether or not it exists. When a CNN model is being trained, the process of selecting the weights and kernels that will produce the most accurate results is referred to as "training the network." It is possible to train an algorithm by making use of a database that is partitioned into three sections. These sections are referred to as training, assessment of the model while it is being trained, and testing of the finished model. In order to train neural networks, a method known as Gradient Descending is utilized, which is explained further on in this article. The performance of the model is evaluated by the optimizer using a loss function in conjunction with a number of filters and weights. When computing error rates, direct propagation is used, but when updating learnable parameters like this one, reverse propagation is what's done. Learnable parameters are updated using a decreasing gradient in order to lessen the likelihood of a person making a mistake. The

step size, which is also referred to as the learning rate or the learning rate in, is what is utilized to update each parameter in such a way that it gets closer and closer to the point where the loss function is at its smallest. An image segmentation algorithm's learning capacity is not only determined by its learning rate, but also by the loss function that is integrated into its overall design. Both of these factors contribute to the algorithm's overall design. The magnitude of the loss value will directly correlate to the degree to which the model's accuracy will suffer. Equation 1 can be used to describe the process of updating the parameters. In this equation, represents the learnable parameters, refers to the learning rate, and L represents the loss function:

$$\omega = \omega - \alpha \cdot \frac{\partial L}{\partial \omega} \qquad (4.2)$$

It is necessary for the program to have the capability of adjusting to a different database in order for it to perform properly. In the course of instruction, a one-of-a-kind section of the database is utilized to validate this estimate of talent. In order to make improvements, it is required to conduct an investigation into the level of precision and the boundaries of the model. When attempting to determine how closely the output of the segmentation algorithm resembles the source image, accuracy is a crucial component that must be taken into consideration. As a direct consequence of this, the voxels that make up each image can be classified according to the following rubrics:

When the algorithm classifies a voxel as "injury," that voxel is referred to as a "True Positive," and when it classifies a voxel as "non-injury," that voxel is referred to as a "True Negative," and when it classifies a voxel as a "False Positive," that voxel is referred to as a "Fals (FN).

5. CONCLUSION AND FUTURE WORK

5.1 CONCLUSION

Textural characteristics can be used to differentiate between different tumor masses in encephalon magnetic resonance imaging. The primary purpose of this investigation is to plan for, create, and carry out a preliminary evaluation of a system that is able to differentiate between two distinct types of tissue, namely tumor and non-neoplastic tissue. This system shouldn't be restricted to analyzing only photographs of a particular sort of tumor; rather, it should be able to deal with a wide range of images representing a number of different cancers. It is possible to partition tumor regions using an approach that is both more efficient and automated by making use of magnetic resonance imaging. This may be accomplished without giving up any of the benefits that have been outlined in earlier sections of this article. The data can be put to use for pre-surgical planning, the production of volumetric visualizations, and, most crucially, the monitoring of any changes that have taken place over the course of time. It is vital to segment the disease in order to determine the efficacy of treatment, determine when the disease began or went into remission, and track its progression. It is not the intention of using computers to segment radiological images of brain tumors in order to do away with the need for a physician; rather, the purpose of doing so is to provide the physician with assistance in his job by completing tasks that are repetitive and mechanical, freeing him up to use his full cognitive capacity. The ability of computer systems to see finer details than the human eye is made possible by the fact that they are not affected by human variables such as weariness or other distractions. The presence of a tumor cell causes a change in the relaxation periods of magnetic resonance, which in turn causes a change in the recorded signal and displays a slight difference in the tissue composition of healthy vs diseased tissues. Alternately, these minuscule variations could be identified through the use of the appropriate mathematical processes.

5.2 DISCUSSION

There is reason to be optimistic about an approach that makes use of information about the tissue's texture in order to differentiate between healthy and malignant tissue. In order to achieve the objective, research that is now being conducted in the appropriate field has resulted in the development of a technique that proposes subdividing tumor tissues into several categories. In our

analysis, we took into account not just newly released publications and books on the subject, but also material that was gained through conversations with well-known authorities in the field. After reviewing the MRI pictures with the intention of evaluating the proposed method, it was necessary to do a biopsy in order to establish whether or not malignancies were present. With the assistance of the library's resources at the Polytechnic School, we were able to successfully complete our investigation. The data collected during the research phase were used to guide the selection of implementation approaches, which ultimately resulted in the development of a prototype that is both functional and contains all of the intended characteristics. Following the conclusion of the implementation, it was time to carry out a thorough investigation of the results. At this point in time, it was more necessary than ever to get in touch with local medical professionals, such as radiologists and oncologists. A comparison was made between images that were segmented by the algorithm and photographs that were segmented manually by cooperating doctors. This comparison formed the basis of this approach of evaluation. We were able to get a good sense of how reliable the findings were by comparing them to other studies that had been done in the past and published that provided a comprehensive analysis of how the measurement was carried out. Magnetic resonance imaging, more commonly referred to as an MRI, is an important diagnostic tool in the fight against brain cancers since it provides anatomical information and is less invasive than other imaging methods. The most accurate method for determining the progression of tumors, surgical planning, and the results of chemotherapy and radiation therapy is magnetic resonance imaging (MRI). Even though tumor segmentation is frequently performed manually, which adds time and effort to the operation, this approach makes it possible to measure both the tumor mass and the patient's response to therapy. This is the case in spite of the fact that manual tumor segmentation typically takes place. It is feasible to determine the extent to which a tumor mass has expanded over the course of time by employing a computer system that allows for manual segmented loading. This was made possible by the introduction of 3D visualization features in MATLAB r2018a, which made it possible for the main purpose of the study to be accomplished. Independent of the input of the user, it is possible to investigate the conclusions that were created from the images of healthy and damaged brains. The findings showed that the suggested system was able to locate tumors and determine the boundaries of the tumors without the need for interaction between the system and the user. On the other hand, the algorithm that was applied in this investigation was successful in creating appropriate segments between automatically separated

parts an average of 91 percent of the time. On the other hand, the average of the negative findings from the CT scans indicates that the size of the tumor was most likely overestimated. For the vast majority of cases, the size of the tumor was overestimated by a significant margin due to one of these four conditions: (high blood pressure and a high positive CT result). In every instance, the area of the tumor was calculated incorrectly. As a result of the absence of histological confirmation of the gold standard, it was not possible to determine with certainty whether there was a mistake in the method or an inaccuracy in the way that the system recognized even minute variations in tissue in the regions around the tumor. This was one of the limitations of the study.

5.3 FUTURE WORK

The importance of the annotations that are contributed to the training database cannot be overstated. Because of the many different factors at play, the segmentation of organs and lesions can be subjective and erroneous at times. There is also the possibility of human error, in addition to the technological constraints that are connected with intramodality registration (when several types of images are used). The "noise" in the ground truth data makes it impossible for it to conduct quantitative evaluations of segmentation algorithms. As a result of this issue, it is unable to do so. Strategies such as those outlined are especially interesting because they make it possible to evaluate the degree of uncertainty associated with segmentation. Within the context of the BRATS challenge, there are three primary categories of tumor tissue: tumor-inducing edema, necrotic core, and contrast enhanced core. Each of these categories is a subtype of the other two. In the course of working on our dissertation, we made use of three distinct types of tumor tissue. The possibility of conducting radiation planning with the help of direct GTV and CTV measurements is quite exciting (CTV). Due to the inability of MRI to differentiate between individual cancer cells, identifying the CTV can be a challenging task. As a consequence of this, the decision will be made by a panel of specialists. In order to automate the computation of CTV, models of tumor growth similar to Angelini's could be applied. We are left with no choice but to treat tumors and organs that are at risk on an individual basis because the datasets that are currently accessible have their limits. It has been ensured that the BRATS challenge will exclusively concentrate on the segmentation of gliomas by the use of preprocessing software on each and every image that will be used in the competition (in particular, the skull has been removed). In the coming years, researchers will continue to concentrate their efforts on tumor segmentation in conjunction with

sensitive organs. Even if there are now a few different segmentation systems available, the vast majority of the time their applications are restricted to specific circumstances and responsibilities. In the long run, while developing new systems, we think it would be desirable to combine a large number of different activities and make use of a variety of different types of data. This is because we feel this would lead to better results. The QN-PSO algorithm and deep learning are both utilized in this research project in order to come up with a revolutionary classification approach for brain tumors. In order to achieve a higher level of contrast between the original photographs, the PSO method, which may also be utilized to create a more accurate QN model, may be utilized. This not only makes the tumor more extensive, but it also reveals previously unknown information. The post-hoc incorporation of features that have a two-layer structure results in an improvement to the original classification accuracy. The approach to classification does take into account redundant qualities; nevertheless, it does not attain the required degree of precision. As a direct result of this, an entirely new algorithm known as the QNPSO has been devised. Because of this, we have arrived at the conclusion that selecting the appropriate attributes will improve classification accuracy while simultaneously reducing the amount of time required for system prediction. A very stringent due date has been imposed on this project, and it is imperative that it gets finished on time. After the urgent matter has been addressed, there is a good chance that the recently implemented capability will function exactly as it was designed to after it has been put into use. One of our goals for the not-too-distant future is to increase the amount of testing that we carry out in addition to enhancing the final finishing criteria for the dataset. As a result of the study, it is feasible to continue analyzing alternative segmentation approaches in order to produce a more comprehensive document that enables subject-matter specialists to reference specific bibliographic support for new research. This is because the study has shown that it is possible to continue analyzing alternative segmentation approaches. This is doable because it is possible to continue evaluating different approaches to segmentation of the data. For the work that will be done in the future, the following recommendations are offered as possible solutions: It is possible to ascertain the precision, sensitivity, and accuracy coefficients of an algorithm by looking for datasets that have a good balance. The many strategies for parameter selection that are now implemented by the clustering (K-means) and swarm optimization (PSO) methods are going to be the subject of an investigation. Think about adding a couple more segmentation approaches if you want the inquiry to cover more ground. 4 Conduct a parallel examination of the metrics that are used to evaluate

these algorithms, and assist in the selection of data that are positioned in a way that is designed to be as comparable as possible to the experimental conditions.

REFERENCES

[1] Bhandarkar M. Automatic brain tumor segmentation. Master's thesis, University of Alberta, 2005.

[2] Bhandarkar S, Koh J, Suk M. Multiscale image segmentation using a hierarchical self-organizing map. Neurocomputing 1997;14:241–72.

[3] Catt J. Chalmers M. Fallowfield C. Minimization of region-scalable fitting energy for image segmentation. IEEE Trans Image Process 2008;17(10):1940–9.

[4] Mirimanoff J, Wang J, Lu Y, Zhang J, Li Y, Zhang B. A novel approach for segmentation of MRI brain images. IEEE MELECON; 2006. p. 525–8.

[5] Bauer Y, Lin Z, Cao J, Li M. Automatic MRI brain tumor segmentation system based on localizing active contour models. Adv Mater Res 2013;2134:219–20.

[6] Behin L, BenyÛ Z, Szilágyi S, Adam H. MR brain image segmentation using an enhanced fuzzy C-means algorithm. Int Conf IEEE EMBS 2003;25: 724–6.

[7] Ali-Osman. An intelligent modified fuzzy C-means based algorithm for bias field estimation and segmentation of brain MRI. Pattern Recognit Lett 2005;26: 2052–62.

[8] Parkin T, Chen, Yang and Cao. Clustering multispectral images: a tutorial. Chemometrics Intell Lab Sys 2005;77:3–17.

[9] Boing; Vargas; Boing C. Segmentation and grading of brain tumors on apparent diffusion coefficient images using self-organizing maps. Comput Med Imaging Graph 2007;31:473–84.

[10] Galanis M, Hall L, Goldgof D, Velthuizen R, Murtagh R, Silbiger M. Automatic tumor segmentation using knowledge-based techniques. IEEE Trans Med Imaging 1998;17(2):187–201.

[11] Pereira M, Abodou M. A neuro-difference fuzzy technique for automatic segmentation of region of interest in medical imaging. NRSC 2016:1–7.

[12] brainard M, Warfield S, Nabavi A, Black P, Jolesz F, Kikinis R. Automated segmentation of MRI of brain tumors. Radiology 2001;218(2):586–91.

[13] grady R, Bischof L. Seeded region growing. IEEE Trans Pattern Anal Mach Intell 1994;16:641–7.

[14] Sing J, Khan K, Basu D, Nasipuri M, Saha P. Polynomial surface fitting based method for retrospective correction of intensity inhomogeneity in MR images. Communications and Signal Processing Intl Conf; 2011. p. 405–9.

[15] Kazerooni A, Ahmadian A, Saberi H, Alirezaie J, Rad H. An efficient algorithm for registration of pre- and intra- operative brain MRI images to correct intensity inhomogeneity. Inf Science, Signal Process and their Applications Intl Conf; 2012. p. 253–8. [

[16] Ho S, Bullitt E, Gerig G. Level set evolution with region competition: automatic 3-D segmentation of brain tumors. Int Conf Pattern Rec 2002;I:532–5.

[17] Prastawa M, Bullitt E, Ho S, Gerig G. A brain tumor segmentation framework based on outlier detection. Med Image Anal 2004;8(3):275–83.

[18] Lee CH, Schmidt M, Murtha A, Bistritz A, Sander J, Greiner R. Segmenting brain tumor with conditional random fields and support vector machines. Computer vision for biomedical image applications; 2005. p. 469–78, http: //dx.doi.org/10.1007/11569541_47.

[19] Dou W, Ruan S, Chen Y, Bloyet D, Constans JM. A framework of fuzzy information fusion for the segmentation of brain tumor tissues on MR images. Image Vis Comput 2007;25:164–71.

[20] Khotanlou H, Colliot O, Atif J, Bloch I. 3D brain tumor segmentation in MRI using fuzzy classification, symmetry analysis and spatially constrained deformable models. Fuzzy Set Syst 2009;160(10):1457–73.

[21] Iftekharuddin K, Zheng J, Islam M, Ogg R. Fractal-based brain tumor detection in multimodal MRI. Appl Math Comput 2009;207:23–41. [22] Gordillo N, Montseny E, Sobrevilla P. A new fuzzy approach to brain tumor segmentation. IEEE Int Conf Fuzzy Sys 2010:1–8.

[23] Vijayakumar C, Gharpure DC. Development of image-processing software for automatic segmentation of brain tumors in MR images.Med Phys 2011;36:147–58.

[24] Bauer Y, Lin Z, Cao J, Li M. Automatic MRI brain tumor segmentation system based on localizing active contour models. Adv Mater Res 2011;2134:219–20.

[25] Kumar D, Halder A. Automatic brain tumor detection and isolation of tumor cells from MRI images. Int J Comput Appl 2012;39(16):26–30.

[26] Papageorgiou E, Spyridonos P, Glotsos D, Stylios C, Ravazoula P, Nikiforidis G, et al. Brain tumor characterization using the soft computing technique of fuzzy cognitive maps. Appl Soft Comput 2008;8:820–8.

[27] Bhandarkar M. Automatic brain tumor segmentation. Master's thesis, University of Alberta, 2005.

[28] Bezdek J, Hall L, Clarke L. Review of MR imaging segmentation techniques using pattern recognition. Med Phys 1993;20(4):1033–48.

[29] Wiselin G, Ganesan L. Unsupervised segmentation using fuzzy logic based texture spectrum for MRI brain images. World Acad Sci Eng Technol 2005;5: 155–7.

[30] Popuri K, Cobzas D, Jagersand M, Shah S, Murtha A. 3D variational brain tumor segmentation on a clustered feature set.SPIE Med Imaging 2009. p. 1–4.

[31] A bertillon, Pernus F, Likar B. A review of methods for correction of intensity inhomogeneity in MRI. IEEE Trans Med Imaging 2007;26(3):405–21.

[32] Hou flom. A review on MR image intensity inhomogeneity correction. Int J Biomed Imaging 2006:1–11.

[33] brainard A, Udupa J. Interplay between intensity standardization and inhomogeneity correction in MR image processing. IEEE Trans Med Imaging 2005;24(5):561–76.

[34] Capelle A Grady, Colot O, Fernandez-Maloigne C. Evidential segmentation scheme of multi-echo MR images for the detection of brain tumors using neighborhood information. Inf Fusion 2004;5(3):203–16.

[35] Violla M, Hall L, Goldgof D, Velthuizen R, Murtagh F, Silbiger M. Unsupervised brain tumor segmentation using knowledge based and fuzzy techniques. Fuzzy and neuro-fuzzy systems in medicine. Boca Raton, FL: CRC Press; 1999. p. 137–69.

[36] phillipset M, Agrawal S. A fully automatic approach to detect brain cancer using random walk algorithm. Int J Comput Technol Appl 2012;3(1):265–8.

[37] Costa KJ, Sasi Kumar M. Skull stripping and automatic segmentation of brain MRI using seed growth and threshold techniques. Conf Intelligent Adv Sys 2007:422–6.

[38] Pauca J, Xue Z, Liu T, Young G, Setayesh K, Guoc L, et al. Automated brain tumor segmentation using spatial accuracy-weighted hidden Markov Random Field. Comput Med Imaging Graph 2009;33:431–41.

[39] leung D, Birkbeck N, Schmidt M, Jagersand M, Murtha A. 3D variational brain tumor segmentation using a high dimensional feature set. Computer Vision, 2007. ICCV 2007. p.1-8, http://dx.doi.org/10.1109/ICCV.2007.4409130.

[40] Farag A, Ahmed M, El-Baz A, Hassan H. Advanced segmentation techniques. Handbook of biomedical image analysis I: segmentation models part A. Springer US; 2005. p. 479–533.

[41] Bondy et C, Pham D, Prince J. Current methods in medical image segmentation. Ann Rev Biomed Eng Ann Rev 2000;2:315–37.

[42] Woodard M, Das A. A study on seeded region based improved watershed transformation for brain tumor segmentation. The XXIX General Assembly of the Int Union of Radio Science; 2008.

[43] Chang H, Valentino D. An electrostatic deformable model for medical image segmentation. Comput Med Imaging Graph 2008;32:22–35.

[44] Park K, Yang J, Zhang Z, Zhu Y. Semi-automated brain tumor and edema segmentation using MRI. Eur J Radiol 2005;56:12–9.

[45] Valetco s P, Buckley D, Blackb S, Horsman A. Tumour determination from MR images by morphological segmentation. Phys Med Biol 1996;41:2437–46.

[46] ChangSun Y, SunHan K, JunSong C, MooNoh S, WonPark J. an evaluation of user-assisted hierarchical watershed segmentation. Med Image Anal 2005:566–78. ICSP2000 2000:1000–9.

[47] Stadlbauer A, Moser E, Gruber S, Buslei R, Nimsky C, Fahlbusch R, et al. Improved delineation of brain tumors: an automated method for segmentation based on pathologic changes of 1H-MRSI metabolites in gliomas. Neuroimage 2004;23:454–61.

[48] grady R, Bischof L. Seeded region growing. IEEE Trans Pattern Anal Mach Intell 1994;16:641–7.

[49] brainard M, Warfield S, Nabavi A, Black P, Jolesz F, Kikinis R. Automated segmentation of MRI of brain tumors. Radiology 2001;218(2):586–91. [50] Salman Y, Badawi A, Assal M, Alian S. New automatic technique for tracking brain tumor response.Int Conf Biol Med Phys 2005. p. 1–4.

[51] zako F, Chong H, Zhou J, James B, Khoo K, Huang J, et al. Tongue carcinoma: tumor volume measurement. Int J Radiat Oncol Biol Phys 2004;59(1):59–66.

[52] Mascerenhas, Badawi A. Validation techniques for quantitative brain tumor measurements. Int Conf IEEE EMBS 2005. p. 7048–51.

[53] Sato M, Lakare S, Wan M, Kaufman A. A gradient magnitude based region growing algorithm for accurate segmentation. Int Conf Image Process 2000;3: 448–51.

[54] Harman S. 3D segmentation techniques for medical volumes. Stony Brooks: Center of Visual Computer, state university of NY; 2015.

[55] Salman Y. Modified technique for volumetric brain tumor measurements. J Biomed Sci Eng 2009;2:16–9.

[56] Cohen J, Hahn H, Klein J, Lentschig M, Peitgen H. Multispectral brain tumor segmentation based on histogram model adaptation. SPIE Conf Med Image Comp, 2017. p. 65140V1-10.

[57] Deng W, Xiao W, Deng H, Liu J. MRI brain tumor segmentation with region growing method based on the gradients and variances along and inside of the boundary curve. Int Conf Biomed Eng Informatics; 2010. p. 393–6.

[58] Letteboer M, Niessen W, Willems P, Dam E, Viergever M. Interactive multi-scale watershed segmentation of tumors in MR brain images. IMIVA workshop of MICCAI; 2001.

[59] Dam E, Loog M, Letteboer M. Integrating automatic and interactive brain tumor segmentation. Int Conf Pattern Rec 2004;3:790–3.

[60] Cates J, Whitaker R, Jones G. Case study: an evaluation of user-assisted hierarchical watershed segmentation. Med Image Anal 2005:566–78.

[61] Ratan R, Sharma S, Sharma SK. Multiparameter segmentation and quantization of brain tumor from MRI images. Indian J Sci Technol 2009;2(2):11–5.

[62] Horowitz A, Leon L. Watershed-based segmentation and region merging. Comput Vis Image Under 1989;77(3):317–70.

[63] Gies V, Bernard T. Statistical solution to watershed over-segmentation. Int Conf Image Process; 2004. p. 1863–6.

[64] HORNAK J, Wang J, Lu Y, Zhang J, Li Y, Zhang B. A novel approach for segmentation of MRI brain images. IEEE MELECON; 19966. p. 525–8.

[65] Bezdek J, Sutton M. Applications of fuzzy systems.Image Process Med 1999 p. 363–416.

[66] Supot S, Thanapong C, Chuchart P, Manas S. Segmentation of magnetic resonance images using discrete curve evolution and fuzzy clustering. IEEE Int Conf Integration Tech; 2007. p. 697–700.

[67] Phillips W, Velthuizen R, Phupanich S, Hall L, Clarke L, Silbiger M. Application of fuzzy C-means segmentation technique for tissue differentiation in MR images of a hemorrhagic glioblastoma multiforme. Magn Reson Imaging 1995;13(2): 277–90.

[68] Galanis M, Hall L, Goldgof D, Velthuizen R, Murtagh R, Silbiger M. Automatic tumor segmentation using knowledge-based techniques. IEEE Trans Med Imaging 1998;17(2):187–201.

[69] Fletcher L, Hall L, Goldgof D, Reed F. Automatic segmentation of nonenhancing brain tumors in magnetic resonance images. Artif Intell Med 2001; 21:43–63

. [70] Veloz A, Chabert S, Salas R, Orellana A, Vielma J. Fuzzy spatial growing for glioblastoma multiforme segmentation on brain magnetic resonance imaging. LNCS 2008;4756:861–70.

[71] Ali-Osman. An intelligent modified fuzzy C-means based algorithm for bias field estimation and segmentation of brain MRI. Pattern Recognit Lett 2005;26: 2052–62.

[72] Kannan S. A new segmentation system for brain MR images based on fuzzy techniques. Appl Soft Comput 2008;8:1599–606.

[73] Szilágyi L, Szilágyi S, BenyÛ Z. A modified fuzzy C-means algorithm for MR brain image segmentation. LNCS 2007;4633:866–77.

[74] Forouzanfar M, Forghani N, Teshnehlab M. Parameter optimization of improved fuzzy c-means clustering algorithm for brain MR image segmentation. Eng Appl Artif Intell 2010;23:160–8.

[75] Tofts, Adam H. MR brain image segmentation using an enhanced fuzzy C-means algorithm. Int Conf IEEE EMBS 2003;25: 724–6.

[76] Chen S, Zhang D. Robust image segmentation using FCM with spatial constraints based on new kernel-induced distance measure. IEEE Trans Syst Man Cybern B Cybern 2004;34:1907–16.

[77] Cai W, Chen S, Zhang D. Fast and robust fuzzy C-means algorithms incorporating local information for image segmentation. Pattern Recognit 2007;40: 825–38.

[78] Parkin T, Wehrens R, Buydens L. Clustering multispectral images: a tutorial. Chemometrics Intell Lab Sys 2005;77:3–17.

[79] Capelle A, Alata O, Fernandez C, Lefevre S, Ferrie J. Unsupervised segmentation for automatic detection of brain tumors in MRI. IEEE Int Conf Image Process 2000:613–6.

[80] Gering D, Grimson W, Kikinis R. Recognizing deviations from normalcy for brain tumor segmentation. Med Image Comput Comput Assist Interv 2002;2488:388–95.

[81] Mazzola J, Xue Z, Liu T, Young G, Setayesh K, Guoc L, et al. Automated brain tumor segmentation using spatial accuracy-weighted hidden Markov Random Field. Comput Med Imaging Graph 2009;33:431–41.

[82] Bauer S, Nolte L, Reyes M. Segmentation of brain tumor images based on atlas-registration combined with a Markov-random-field lesion growth model. IEEE Int Symp Biomedical Imaging: From Nano to Macro; 2011. p. 2018–21.

[83] Zhang J, Ma K, Er M, Chong V. Tumor segmentation from magnetic resonance imaging by learning via one-class support vector machine. Int Workshop Adv Image Technol 2004:207–11.

[84] Clarke L. MR image segmentation using MLM and artificial neural nets. Med Phys 1991;18(3):673.

[85] Ozkan M, Dawant B, Maciunas R. Neural-network-based segmentation of multi-modal medical images: a comparative and prospective study. IEEE Trans Med Imaging 1993;12(3):534–44.

[86] Dickson S, Thomas B. Using neural networks to automatically detect brain tumours in MR images. Int J Neural Syst 1997;4(1):91–9.

[87] Pereira M, Abodou M. A neuro-difference fuzzy technique for automatic segmentation of region of interest in medical imaging. NRSC 2016:1–7.

[88] Boing; Vargas; Boing C. Segmentation and grading of brain tumors on apparent diffusion coefficient images using self-organizing maps. Comput Med Imaging Graph 2007;31:473–84.

[89] Reddick W, Glass J, Cook E, Elkin T, Deaton R. Automated segmentation and classification of multispectral magnetic resonance images of brain using artificial neural networks. IEEE Trans Med Imaging 1997;16(6):911–8.